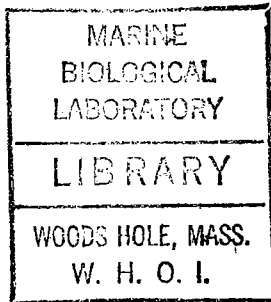THE MARINE

GEOCHEMISTRY

OF TRACE METALS

by

EDWARD ALLEN BOYLE

B.A., University of California, San Diego

(1971)

SUBMITTED IN PARTIAL FULFILLMENT OF THE
REQUIREMENTS FOR THE DEGREE OF
DOCTOR OF PHILOSOPHY

at the

MASSACHUSETTS INSTITUTE OF TECHNOLOGY

and the

WOODS HOLE OCEANOGRAPHIC INSTITUTION

April, 1976

Signature of Author.... *Ed Boyle* ....
        Joint Program in Oceanography, Massachusetts
        Institute of Technology - Woods Hole Oceanographic
        Institution, and Department of Earth and Planetary
        Sciences, Massachusetts Institute of Technology
        April, 1976

Certified by..
                              Thesis Supervisor

Accepted by..
        Chairman, Joint Oceanography Committee in the
        Earth Sciences, Massachusetts Institute of
        Technology - Woods Hole Oceanographic Institution

THE MARINE GEOCHEMISTRY OF TRACE METALS

by

EDWARD ALLEN BOYLE

Submitted to the Joint Oceanographic Committee of
the Department of Earth and Planetary Sciences,
Massachusetts Institute of Technology, and the
Woods Hole Oceanographic Institution on April 16,
1976, in partial fulfillment of the requirements
for the degree of Doctor of Philosophy.

ABSTRACT

The marine geochemical cycles of iron, copper, nickel,
and cadmium were studied in order to provide a basis for
oceanographic models for trace metals.

Copper, nickel, and cadmium can be determined in a
100 ml seawater sample using cobalt pyrrolidine dithio-
carbamate chelate coprecipitation and graphite atomizer atomic
absorption spectrometry. Concentration ranges likely to
be encountered and estimated (1σ) analytical precisions
are copper, 1 to 6 nanomole/kg (± 0.1); nickel, 3 to 12
nanomole/kg (± 0.3); and cadmium, 0.0 to 1.1 nanomole/kg (± 0.1).
The technique may be applied to freshwater samples with
slight modification.

A survey of several east coast U.S. estuaries established
that an iron removal process occurs commonly when rivers mix
with seawater. Laboratory mixing experiments using water
from the Merrimack River (Mass.) and the Mullica River
(New Jersey) demonstrated that rapid iron precipitation
occurs as negatively-charged iron-organic colloids react
with seawater cations and coagulate. This phenomenom was
modeled using a synthetic, organic-stabilized colloidal
suspension of goethite. The generality of the mechanism
suggests that the world-average net river input of iron
to the oceans is less than 1 μmole/kg of river water, an
order of magnitude below previous estimates.

Profiles of cadmium were obtained for 3 GEOSECS stations
in the Pacific Ocean. Cadmium shows a consistent
linear correlation with phosphate which demonstrates that
cadmium is regenerated in a shallow cycle within the water
column. The water column correlation is consistent with data
on cadmium in marine organisms. Cadmium is enriched in upwelling
regions which explains reports of cadmium enrichment in plankton
from the Baja California upwelling region.

Copper and nickel measurements have been made for three
profiles from the Pacific Ocean. Observed copper concentrations
range from 1 to 6 nanomole/kg; nickel varies from 3 to 12
nanomole/kg. Copper and nickel are removed from surface
waters by uptake into organisms. As noted previously, nickel
is regenerated partially in a shallow cycle (like P) and also

in a deep cycle (like Ba). Copper is regenerated from biological debris at the bottom but is also scavenged from the mid and deep water column by an undetermined mechanism. The scavenging residence time is 1400 years. An estimate for the continental input of Ni, 7 nanomole/kg of river water, and Cu, 18 nanomole/kg of river water, was derived from measurements in the Amazon estuary. The oceanic residence times for nickel and copper are about 10,000 years.

Evidence available on the uptake laws for trace metals by plankton suggests that a consistent relationship between the uptake law and the depth of regeneration may apply.

THESIS SUPERVISOR: Professor John M. Edmond, M.I.T.

DEDICATION

To Vikki and my parents

ACKNOWLEDGEMENTS

TABLE OF CONTENTS

LIST OF FIGURES

List of figures (Cont'd)

LIST OF TABLES

NOTE ON REFERENCES:

To facilitate publication, the references for a given chapter are listed at the end of each chapter rather than collected at the end of the entire thesis.

Chapter 1

Introduction

Transition elements display a remarkable diversity of chemical properties and participate in a variety of interesting geochemical processes. Most of what is known about these metals in the marine geochemical cycle has come from the study of sediments and manganese nodules, with little information available on their distribution in the overlying water column. Yet the ocean is a source for sediments and is the medium for the transportation of particles to the sea floor. Attempting to understand the distribution of transition metals in sediments w_thout knowing their behavior in the water column is analagous to examining the distribution of siliceous sediments without information on the variations of silicate throughout the ocean.

Broecker's recent chemical oceanography textbook (1) contained an "oceanographic periodic table" of elements for which there was at least a first-order understanding of the oceanic distributions. The table has a strange appearance to those familiar with the usual chemical periodic table: all of the transition elements were missing. As discussed in a later chapter of the same book, the reason that these elements are missing is that the levels encountered are so low that they defy accurate measurement. Not only are analytical problems encountered, but the task requires sampling water of low concentration in an

environment (ships, hydrowire, messengers, even "metal-free" plastic samplers) abounding in these elements.

An extensive survey of the literature on water-column transition metal distributions has been given by Brewer (2). This literature will not be elaborated on here as the aforementioned problems with analysis and contamination invalidate most of the data. But three significant steps towards progress in the field should be mentioned. Richards (3) pointed out that tables of the trace chemical composition of seawater so widely quoted and used indiscriminately in calculations and experiments were based on few and often contradictory analyses and were probably meaningless. Subsequently Shutz and Turekian (4) undertook to determine the geographical and vertical distributions of a large number of trace elements. Their major contribution lay in recognizing that knowledge of the distribution under a wide variety of oceanographic conditions was essential to understanding the mechanisms controlling the variations. Finally the GEOSECS test cruises introduced the technique of detailed vertical profiling and simultaneous measurement of numerous oceanographic properties chemical properties to the field of trace metal geochemistry (5). This eventually led to the concept that oceanographic consistency is the primary criterion of the validity of data (6). Physical processes of circulation smooth out variations and the transition metals cannot be more erraticly

distributed than other properties. This criterion made
it clear that there were serious problems with then-available
techniques of sampling and analysis and inspired the
development of improved procedures.

The concentration levels of various elements in the
ocean are the resultant of a dynamic balance between
processes of supply and removal. In view of the difficulties
encountered in the analysis of seawater for trace species
it may be expected that estimates of the river supply are
subject to similar caveats. The most extensive compilations
of river trace metal concentrations are those of Durum et.
al. (7) and Turekian (8). Although there is no definite
evidence that these estimates are erroneous, data based
on new techniques should be obtained.

Another reason for reassessing the continental input
of trace metals is the occurence of reactions in estuaries
which alter the primary river flux. Kharkar et. al. (9)
suggest that desorption reactions can alter significantly
the net continental input. In fact, desorption has been
observed for barium in the Mississippi estuary with a
factor of two increase in the dissolved barium input (10).
Removal of iron has been reported for a few estuaries
(11,12,13) with a decrease in the net supply of 50% or
more. In view of such reactions, investigation of the
flux of materials through estuaries is an essential part
of a study of the marine geochemistry of trace metals.

The following chapters discuss aspects of the marine

geochemistry of a few transition metals: (1) the estuarine
geochemistry of iron, copper, and nickel, and (2) the
water-column distributions of copper, nickel, and cadmium.
The assymetry here - that is, no estuarine chemistry for
cadmium and no water column distribution for iron - is
testimony for some yet-unsolved problems of technique.

References

(1) Broecker, W.S. (1974), Chemical Oceanography, Harcourt, Brace, Jovanovich, Inc, New York, 214 p.

(2) Brewer, P.G. (1975), Minor elements in seawater, in: Chemical Oceanography, second edition, J.P. Riley and G. Skirrow, eds., Vol. 1, Ch. 7, p. 415.

(3) Richards, F.R. (1956), On the state of our knowledge of trace elements in the ocean, Geochim. Cosmochim. Acta 10:241-243.

(4) Schutz, D.F. and K.K. Turekian (1965), The investigation of the geographical and vertical distribtuion of several trace elements in seawater using neutron activation analysis, Geochim. Cosmochim. Acta 29:259-313.

(5) Spencer, D.W.,D.E. Robertson, K.K. Turekian, and T.R. Folsom (1970), Trace element calibrations and profiles at the GEOSECS test station in the Northeast Pacific Ocean, J. Geophys. Res. 75:7688-7696

(6) Boyle, E.A. and J.M. Edmond (1975), Copper in surface waters south of New Zealand, Nature 253: 107-109.

(7) Durum, W.H. and J. Haffty (1963), Implications of the minor element content of some major streams of the world, Geochim. Cosmochim. Acta 27:1-11.

(8) Turekian, K.K. (1971) Rivers, Tributaries, and Estuaries, in: Impingement of Man on the Oceans (ed. Hood), Wiley, p.9-73.

(9) Kharkar, D.P., K.K. Turekian, and K.K. Bertine (1968), Stream supply of dissolved silver, molybdenum, antimony selenium, chromium, cobalt, rubidium, and cesium to the oceans, Geochim. Cosmochim. Acta 32:285-298.

(10) Hanor, J. and L.H. Chan (1975), Behavior of barium during mixing of Mississippi river and Gulf of Mexico water, Geol. Soc. Am. abstracts 7 :1098-1099.

(11) Coonley, L.S., E.B. Baker, and H.D. Holland (1971) Iron in the Mullica River and in Great Bay, New Jersey, Chem. Geol. 7:51-63

(12) Windom, H.L., K.C. Beck, and R. Smith (1971), Transport of trace elements to the Atlantic Ocean by three southeastern rivers, Southeast. Geol. pp. 1109-1181.

(13) Boyle, E.A., R. Collier, A.T. Dengler, J.M. Edmond, A.C. Ng, and R.F. Stallard (1974), On the chemical mass-balance in estuaries, Geochim. Cosmochim. Acta 38:1719-1728.

Chapter 2

Determination of Copper, Nickel, and

Cadmium in Seawater

Introduction

This report describes a technique for the determination of copper, nickel, and cadmium in seawater. The metals are concentrated from a 100 ml sample by cobalt pyrrolidine dithiocarbamate coprecipitation (1). The precipitate is redissolved in an organic solvent and digested to simplify the sample matrix. The resulting solution is analyzed using heated graphite atomizer flameless atomic absorption spectrometry. Extension of the method to freshwater samples is discussed briefly.

Method

An adequate analytical method for analyzing elements at very low concentration levels must preclude contamination of the sample during analysis as well as satisfy accuracy and sensitivity requirements. An elaborate clean-room technique entails considerable inconvenience in terms of cost and availability and does not entirely eliminate possible introduction of contamination by the analyst. For this reason the method was designed to be practicable in an ordinary laboratory with the precautions outlined below.

(1) Reagents are stored in polyethylene or polyproplylene bottles leached in 1 N hydrochloric acid for at least one day. For acid storage, bottles are leached in 6 N hydrochloric acid at 80°C for 2 hours. When not in use, bottles are covered with plastic bags.

(2) All glassware and plasticware used in the analysis are
     stored in a covered bath with a leaching solution con-
     sisting of 0.1 N hydrochloric acid and 0.1 N nitric
     acid. Immediately prior to use, the glassware is
     rinsed with high purity distilled water and used
     without drying. The distilled water should be of
     sufficient purity to give no detectable blank if
     treated as a sample.

(3) Disposable polyethylene gloves are used for critical
     handling steps.

(4) Samples are allowed minimal exposure to open laboratory
     air.

(5) Microliter pipette tips are flushed several times with
     0.1 N hydrochloric acid before each use.

(6) Silicone rubber stoppers are used and kept in 2% EDTA
     solution between each use.

Other precautions will be mentioned in the procedure
description. Although not used in this investigation, a
laminar flow clean bench would help ensure integrity of
the sample during manipulation steps and is recommended.

Two special items used in the procedure are illustrated
in Fig. 1. The filtration funnel (A) is made by joining a
15 ml fine grade sintered glass frit to the bottom of a
tall-form 200 ml pyrex beaker. The dissolution apparatus
(B) is made from plexiglass and silicone rubber stoppers.

Figure 2-1.

        A) Filtration Funnel

        B) Dissolution Apparatus

A

200 ML
TALL FORM BEAKER

15 F
FRITTED FUNNEL

B

SILICONE RUBBER STOPPER

TO VACUUM

5 ML
TEFLON BEAKER

PLEXIGLAS FRAME

SILICONE RUBBER STOPPER
(PARTIALLY HOLLOW)
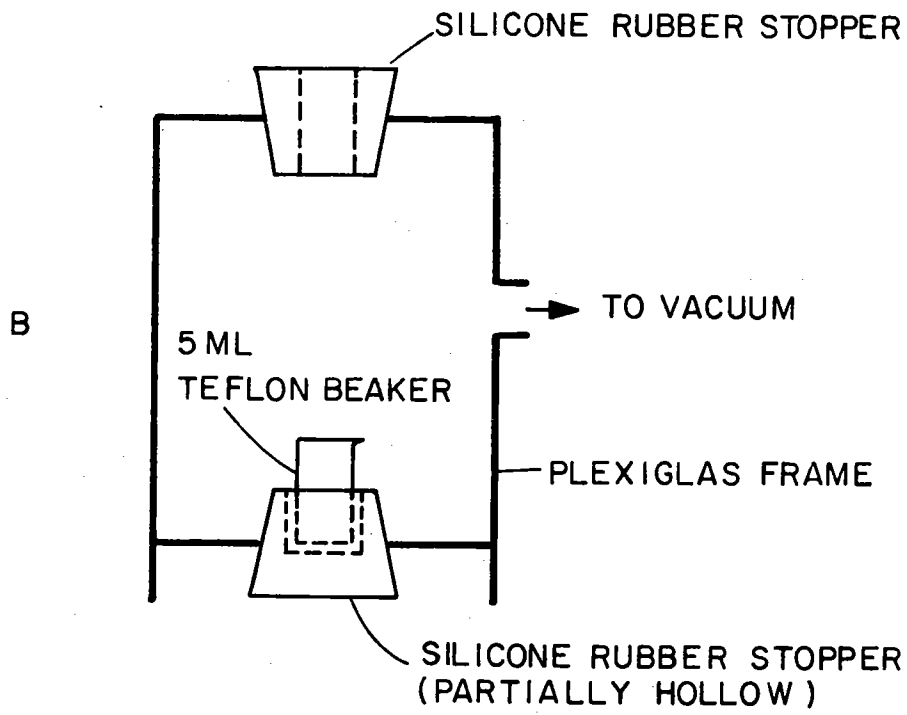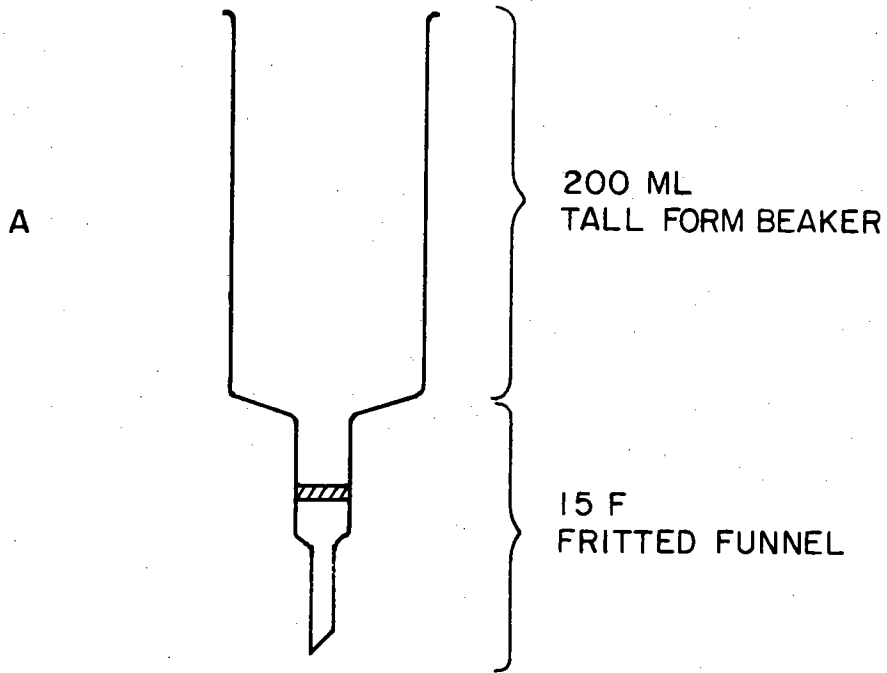
Additionally, a frame for securing the filtration funnel
into a 250 ml filter flask is necessary; this frame
may be constructed from plexiglass using 1/8" OD tygon
tubing straps with glass hooks.

The following reagents are used:

(1) cobalt chloride solution: 0.2 g ultrapure $CoCl_2 \cdot 6H_2O$ dissolved in 250 ml of distilled water.

(2) APDC solution: 2% ammonium pyrrolidine dithio-
carbamate (2) solution purified by repeated solvent
extraction with carbon tetrachloride.

(3) acid acetone mixture: acetone plus 5% b·· volume
0.1 N hydrochloric acid, dispensed with a 250 ml
polyethylene squeeze bottle.

(4) nitric-perchloric acid mixture: 6 N nitric acid,
redistilled in a vycor glass still with 1% by
volume ultrapure perchloric acid.

(5) 0.1 N hydrochloric acid.

(6) acid ammonium sulfate solution: 3×10^{-2} N reagent
grade ammonium sulfate with 3×10^{-2} N reagent
grade sulfuric acid.

(7) 6 N hydrochloric acid, redistilled in a vycor glass
still.

(8) standards: 20 μmol/ml nickel and copper standards
and 10 μmol/ml cadmium standard in 0.1 N hydrochloric
acid.

Samples should be acidified to pH = 2 by addition of

ὖ N hydrochloric acid immediately after collection. This

procedure minimizes adsorption onto container walls (3).

Analytical procedure:

(1) Weigh out approximately 100 g of sample into a

200 ml tall form beaker.

(2) Add 250μl cobalt chloride solution and swirl

gently to mix thoroughly.

(3) Add 500μl APDC solution, swirl gently to mix

thoroughly, and allow the precipitation to procede for 5

minutes before filtration. During this waiting period,

(4) Remove the filtration funnel from the acid bath,

rinse with distilled water, and strap into the filtration

rig. Apply full vacuum and rinse the interior of the

filtration funnel with two portions of 6N hydrochloric acid

followed by two portions of distilled water. After the

5 min. reaction period;

(5) Filter the sample using full vacuum. After the

sample is completely filtered, rinse the interior of the

funnel with a small portion of distilled water to remove the

last traces of sea salt. Then release the vacuum slowly by

means of a stopcock valve with an in-line air filter.

(6) Remove a 5 ml teflon beaker from the acid bath and

rinse with distilled water. Place it into the dissolution

apparatus. Rinse the bottom tip of the filtration funnel

with acid acetone and place the funnel into the top of the

dissolution apparatus. Rinse through several small portions
of acid-acetone mixture by applying a gentle vacuum. This
procedure will dissolve the precipitate and wash it into the
beaker. Release the vacuum; remove the beaker, and care-
fully remove the filter funnel from the dissolution apparatus.
Remove the traces of the chelate from the tip of the filter
funnel by washing the tip with acid-acetone mixture and
collecting the wash in the teflon beaker.

(7) Cover a hot plate with a glass fiber filter. Place
the beaker on the hot plate at very low heat (to avoid
bumping) and cover with an inverted 20 ml pyrex beaker; the
glass fiber minimizes spattering of condensate running down
the inside of the cover. Tilt the beaker by placing one
edge on a glass rod: this prevents condensation from falling
back into the beaker. Evaporate to dryness.

(8) Add 500µl of nitric-perchloric mixture and evaporate
to dryness at slightly higher heat. Avoid charring the
residual organic material by overheating. Upon cooling, the
beaker may be covered with parafilm (R) and stored indefin-
itely.

(9) In addition to evaporation of the samples, a matrix
for standards is prepared by pipetting 250µl of cobalt
chloride solution into each of three 5 ml beakers, adding
10µl APDC solution to each, and proceeding through steps
(7) and (8).

(10) Blanks are determined by running high-purity
water as a sample. The water may be tested for traces of

the metals by varying the volume of several blank samples.

(11) About one hour before the atomic absorption analysis is to be commenced, pipette 2000µl of 0.1 N hydrochloric acid to each sample and standard matrix beaker. While allowing 15 minutes for the residue to dissolve, prepare a secondary mixed standard by diluting 10µl cadmium standard plus 50µl copper standard and 100µl nickel standard to 100.0 ml with distilled water. Mix thoroughly and pipette 50µl into one of the standard matrix beakers and 100µl into another. The third matrix beaker is used for a matrix blank. After the dissolution period, swirl each beaker gently to mix the solution and rinse the sides of the beaker. This solution is used for copper and nickel analyses.

(12) Prepare a diluted solution for cadmium analysis by pipetting 250µl from each concentrated sample and standard into a dry 5 ml teflon beaker. Add 750µl of acid ammonium sulfate solution and mix by gentle swirling. Cover all beakers with parafilm and analyze immediately to minimize evaporation.

Determinations are made using a Perkin Elmer HGA 2100 graphite furnace, model 403 atomic absorption spectrophotometer and model 56 chart recorder. Manufacturer's recommended operating conditions for wavelength, slit and lamp current are followed. Instrumental parameters for the graphite furnace are given in Table 1. Deuterium arc simultaneous background correction is applied, with the deuterium arc beam aligned to coincide with the hollow

Table 1 Instrumental Parameters for HGA-2100

Element	Sample Volume	Gas flow continuous	Dry Cycle	Char cycle	Atomization cycle	High-temperature cleaning cycle
Cu	50	30 cc/min	25 sec @ 110°C	20 sec @ 850°C	10 sec @ 2400°C	-
Ni	100	30 cc/min	35 sec @ 110°C	20 sec @ 1150°C	12 sec @ 2600°C	-
Cd	50	20 cc/min	25 sec @ 110°C	20 sec @ 500°C	5 sec @ 1600°C	5 sec @ 2000°C

cathode beam at the center of the graphite tube. Optical
windows are kept clean using recommended cleaning procedures
and are masked outside of the optical path to minimize light
scattering in the optics. The chart recorder is set to
0.5 absorbance full scale with minimum pen damping. Typical
peak height output is illustrated in Fig. 2. A 100 g sample
with 1 nmol/kg of each element processed as described above
should give peak absorbances of approximately 0.02 for
copper, 0.01 for nickel, and 0.1 for cadmium.

All samples and standards are injected in duplicate or
more if duplicates disagree significantly. Standards are
run before and after each series of about five samples and
a drift correction is applied to concentration calculations.
The volumes and standard concentrations have been chosen to
remain within the linear range. The use of two standards of
different concentrations spanning the absorbance range is
recommended to verify linearity and correct for slight non-
linearity which may occasionally occur with some graphite
tubes. On at least one occasion it is advisable to run a
detailed standard curve to determine where departures from
linearity become significant. The experience from this
investigation suggests that the curve is reliably linear
below an absorbance of 0.15.

The cobalt chloride should be sufficiently pure that
the standard matrix blank gives a peak height < 0.5
milliabsorbance. Where a small matrix blank is observed,

Figure 2-2. Representative peak height output

for copper, nickel, and cadmium.

Duplicate injections are indicated

by brackets. Peak height expected

for 1 nmol/kg (Cu, Ni) and 0.1

nmol/kg (Cd) in a 100 g sample

is indicated by bar.
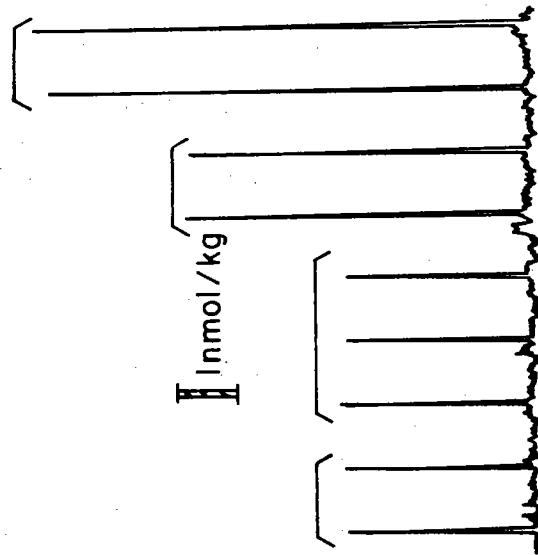
COPPER
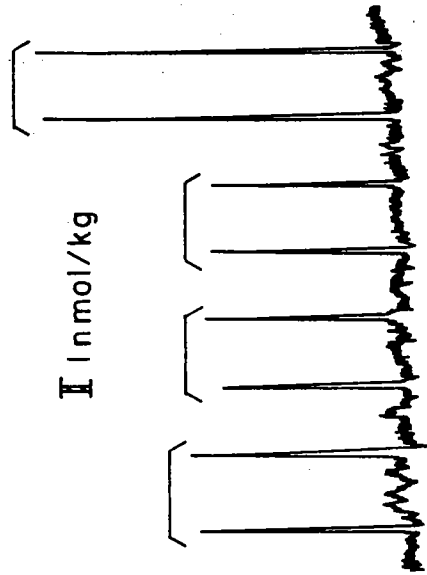
NICKEL
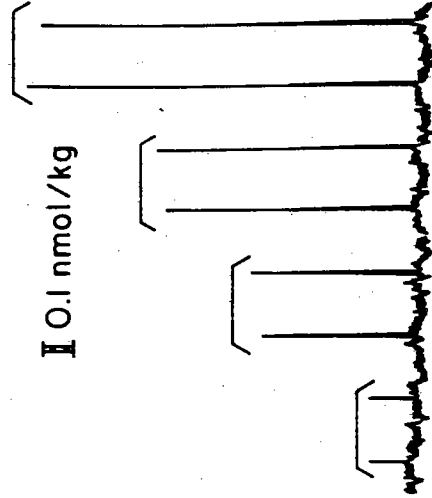
CADMIUM

this value is subtracted from the peak heights of the standards. With some instruments a small (<1 milliabsorbance) baseline shift occurs upon atomization; if necessary this correction should also be applied to the peak signals.

The precision of duplicate injections is highly dependent on the degree to which pipetting into the furnace is performed reproducibly. Satisfactory results can be obtained using Brinkmann pipette tips by gently inserting the pipette tip into the graphite tube as far as possible (Fig. 3). The tip is then in precisely the same position for each injection.

It is advisable to monitor the recovery efficiency periodically by standard additions. The recovery is quite reproducible, however, and need not be determined for each sample.

Results

Two standard addition curves for a deep Sargasso Sea water sample are shown in Fig. 4. Average recovery efficiencies from these curves are copper 106%, nickel 102%, and cadmium 91%. Copper and nickel recoveries are not significantly different from quantitative, whereas cadmium recovery is about 10% lower. Table 2 gives the results of duplicate analyses on water samples taken from a profile at a station south of New Zealand (GEOSECS station 293). The pooled standard deviations are copper ±0.13 nmol/kg, nickel ±0.28 nmol/kg, and cadmium ±0.10 nmol/kg. A comparison of copper analyses by this technique with flame atomic

Figure 2-3. Technique for reproducible pipetting into graphite tube.

EPPENDORF TIP

GRAPHITE
TUBE

SAMPLE DROPLET
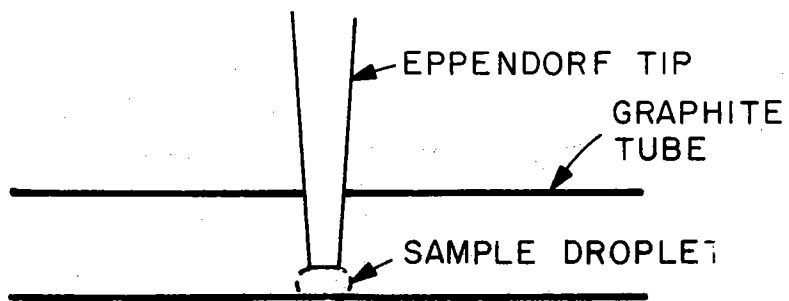
Figure 2-4. Standard additions curve for a

seawater sample.

CADMIUM RECOVERED, nmol/kg

CADMIUM ADDED, nmol/kg

NICKEL RECOVERED, nmol/kg

NICKEL ADDED, nmol/kg

COPPER RECOVERED, nmol/kg

COPPER ADDED, nmol/kg
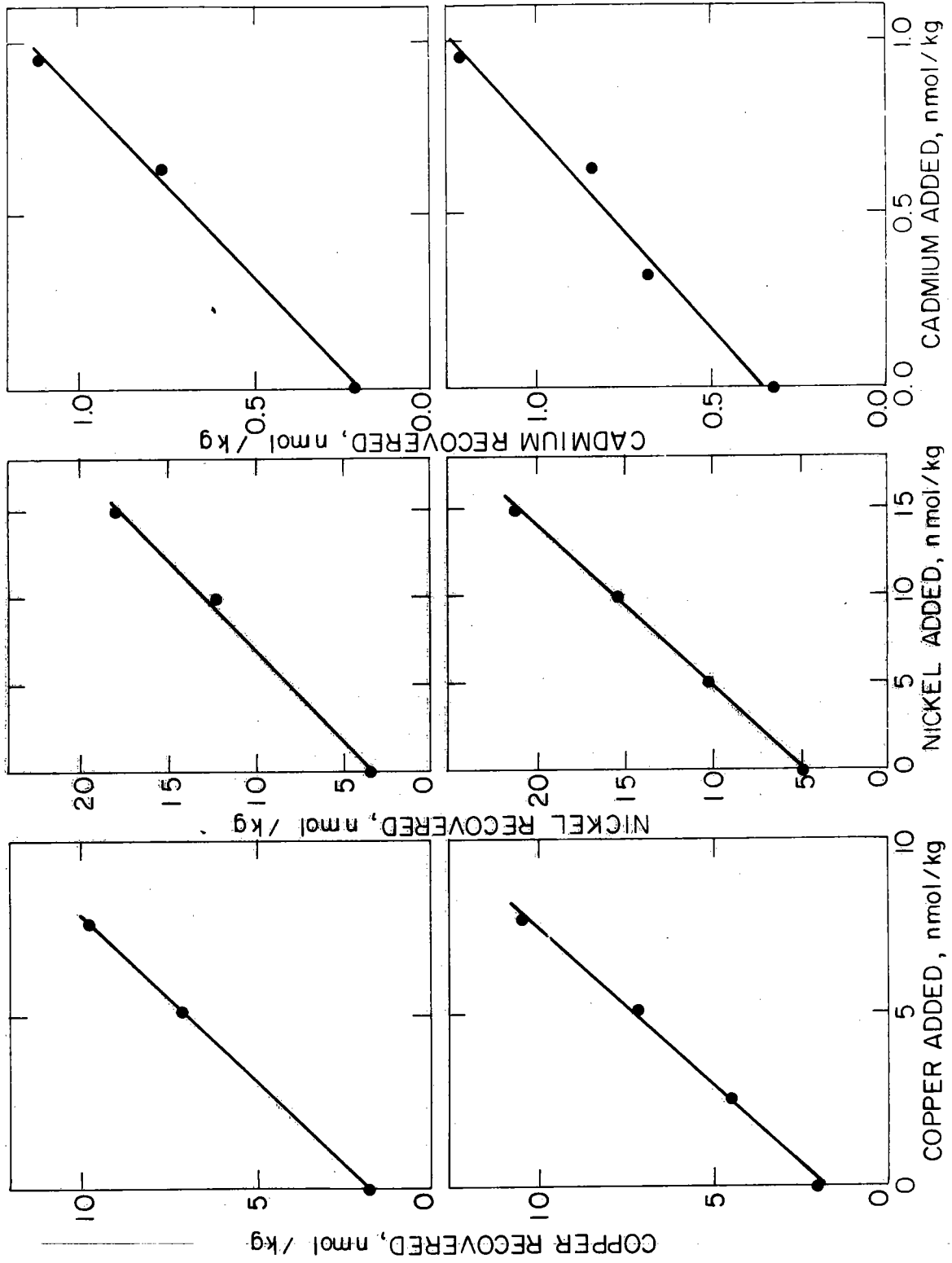
Table 2 Replicate Seawater Analyses

Sample Depth	Copper	Nickel	Cadmium
216 m	1.28 nmol/kg 1.14	4.5 nmol/kg 4.7	0.31 nmol/kg 0.38
916 m	2.48 2.17	5.8 6.2	0.71 0.73
1733 m	2.25 2.19	7.2 7.1	0.87 —
2326 m	2.85 2.63 2.74	7.8 7.0 7.1	1.07 1.12 1.29
4926 m	4.55 4.08	8.2 7.8	0.98 1.26
Pooled Standard Deviation	0.13	0.28	0.10

absorption analyses using a similar coprecipitation technique (1,4) is given in Table 3. The results from the two methods agree within the estimated errors of the methods and rule out a systematic error unique to either flame or flameless analysis.

The accuracy of the analysis is estimated to be comparable to the precision. The results of the standard additions tests suggest an accuracy for the determination of added Cu, Ni, and Cd of better than 10%. No suitable reference standard seawater samples are available for comparison, however.

The limiting factor in the precision of the analysis is not the atomic absorption determination. This conclusion is based on a comparison of the pooled precision of duplicate injections with the overall precision (Table 4). In each case the precision of duplicates is better than the overall precision. For copper and nickel the limiting factor in the precision is probably quantitative transfer of the precipitate into the final solution. For cadmium there may be an additional error associated with the slightly lower (and therefore potentially more variable) precipitation recovery efficiency. Improvements in the precision of this analysis should be sought through improvements in the sample handling procedure rather than in the analytical instrumentation.

Table 3   Comparison of Flame and Flameless Atomic
Absorption Analyses of Seawater Samples

Sample #*	Flameless	Flame	Δ Flameless-flame
284	1.80 nmol/kg	1.80 nmol/kg	0.00
290	1.99	1.87	0.12
292	1.35	0.98	0.37
293	1.50	1.33	0.17
294	1.39	1.28	0.11

The average Δ is 0.15, consistent with the estimated precisions

of 0.13 (flameless) and 0.15 (flame)

*See reference (4) for description of samples.

Table 4. Comparison of precision of duplicate
          samples (table 2) with duplicate injections

Element	Pooled Standard Deviations	
	Duplicate Samples	Duplicate Injections
Cu	0.13 nm/kg (n=6)	0.04 nm/kg (n=25)
Ni	0.28 (n=6)	0.10 (n=19)
Cd	0.10 (n=5)	0.03 (n=22)

Discussion

The analytical technique described above is the result of a series of optimization experiments which will not be described in detail here. However, some of the preliminary work with cadmium will be described to illustrate the methodology of optimization and some of the reasons for the recommended procedure. Cadmium is used as the example because it exhibited the largest variations with respect to changes in analytical conditions.

Initial work showed that cadmium displays interference effects in the presence of cobalt. Injection of a standard in a cobalt chloride matrix resulted in rapidly decreasing peak absorbance on successive injections, using a char temperature of 300°C and atomization temperature of 1600°C. When this series of injections was followed by a high-temperature (2600°C) tube cleaning cycle for 10 seconds, the sensitivity was restored to its initial level. Apparently cobalt coats the graphite surface and retards reduction of cadmium to the atomic state. The high temperature cycle removes cobalt and allows reduction to proceed unhindered. Similar coating effects have been used to minimize carbide formation (5). In addition to this cumulative coating effect, cobalt also affects the peak height of cadmium in a cleaned tube (Fig. 5a,b). Use of a higher atomization temperature does not eliminate this effect (Fig. 5c). Error from this

Figure 2-5.

A) Effect of $(Co) = 10^{-3.1}$M on cadmium

standard curve

B) Effect of cobalt concentration on

cadmium peak height at 1600°C atomization

temperature.

C) Effect of atomization temperature on

cobalt interference, $(Co) = 10^{-3.1}$M,

$(Cd) = 115$ nmol/liter.
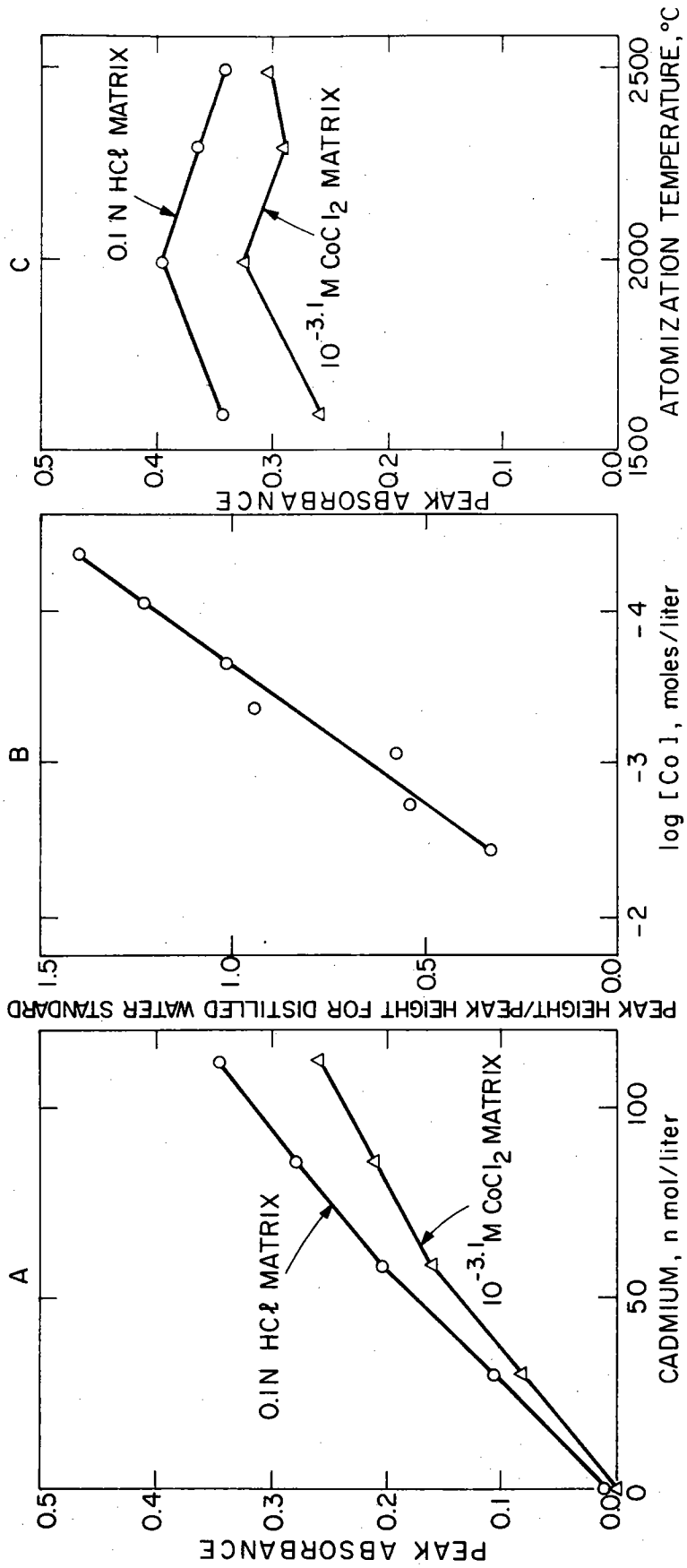
source can be eliminated by using standards containing the same cobalt concentration as the samples. Sensitivity is enhanced by minimizing the amount of cobalt used in the precipitation procedure and by dilution of the final concentrate. Finally, addition of ammonium sulfate to the matrix allows the use of a higher charring temperature (6) and minimizes interferences.

The coprecipitation procedure is applicable to fresh water samples also with the following modifications. Fresh water dissolved organic material will often precipitate upon acidification and clog the fritted glass discs in a short time. To avoid this problem a filter rig utilizing disposable acid-leached glass fiber filters should be substituted for the filtration funnels. For some highly-colored water samples, the organic material inhibits precipitation at the reagent levels recommended above. If this effect is observed, the cobalt and APDC levels should be increased until the chelate does not pass through the filter. The recovery efficiency should be monitored for each different sample type.

Conclusions

APDC chelate coprecipitation coupled with flameless atomic absorption provides a simple and precise analytical method for the determination of nanomole/kg levels of copper, nickel, and cadmium in seawater. With practice, the method

is not overly time-consuming. It is reasonable to expect

to complete sample concentration in less than 20 minutes,

and atomic absorption analysis time should average about

5 minutes per element. Excellent results have been obtained

on the distribution of nickel in the ocean using this

technique (7).

References

1. Boyle, E.A. and J.M. Edmond (1975) Determination of
    trace metals in aqueous solution by APDC chelate
    coprecipitation in Analytical Methods in Oceanography
    (ed. Gibb) Advances in Chemistry Series No. 147,
    American Chemical Society, Washington, pp. 44-55.

2. Slavin, W. (1968), Atomic Absorption Spectroscopy, p. 75,
    Interscience.

3. Robertson, D.E. (1968), The adsorption of trace elements
    in seawater on various container surfaces, Anal. Chim.
    Acta 42: 533-536.

4. Boyle, E.A. and J.M. Edmond (1975), Copper in surface
    waters south of New Zealand, Nature 253: 107-109.

5. Runnels, J.H., R. Merryfield, and H.B. Fisher (1975),
    Analysis of petroleum for trace metals - a method for
    improving detection limits for some elements with the
    graphite furnace atomizer, Anal. Chem. 47: 1258-1263.

6. Ediger, R.D. (1975) Atomic absorption analysis with the
    graphite furnace using matrix modification, At. Abs.
    Newsletter 14: 127.

7. Sclater, F.R., E.A. Boyle, and J.M. Edmond (1976) On
    the Marine Geochemistry of Nickel, Earth Plan. Sci.
    Lttrs. , in press.

Chapter 3

The Mechanism of Iron Removal in Estuaries

Introduction

The great diversity of behavior displayed by iron gives it excellent potential as an indicator of past environments and has inspired much work to elucidate its geochemical cycle. The distribution of iron between various particulate and dissolved forms in rivers in large measure determines the pathways iron will follow in the ocean. Although the transport mechanisms for river-borne particulate iron are understood in a general way (Carroll,1958; Strachov, 1948 - quoted in Livingstone, 1963), there is little agreement on the chemical nature of "dissolved" iron.

In the following discussion iron that passes through filters of specified pore size will be referred to as being "in solution"; no rigorous physical-chemical definition of the dissolved state is intended to apply to this operational definition.

Iron concentrations typically found in freshwater systems exceed by far the levels expected for inorganic dissolved iron species in equilibrium with stable solid phases (Jones et al., 1974). This fact has been explained most frequently as being due either to dissolved organic matter which forms complexes with iron and raises its solubility, or to colloidal iron oxide particles which remain in solution after filtration or centrifugation.

The transport properties predicted by the two hypotheses are quite similar in river systems, but the reactivity of the iron should be quite different once it reaches the sea.

There is evidence for removal of iron from solution in
a few estuaries (Coonley et al., 1971; Windom et al., 1971;
Boyle et al., 1974; Bewers et al., 1974). If this process
is widespread, the input of iron to the ocean will be
reduced considerably from the primary river flux. The
geochemical cycles of other elements may also be affected,
especially should the process involve precipitation of
hydrated ferric oxide, an efficient chemical scavenging
agent. Therefore an understanding of the chemical nature
of iron in rivers and its reactivity in estuaries is essential
to the construction of the marine geochemical cycle of iron
and other trace elements.

Recent literature on the iron-organic association and the
colloidal properties of iron oxide is summarized in Table 1.
The question of the chemical form of iron in rivers cannot
be resolved with certainty from this body of information
because most studies were not designed to rule out alternate
hypotheses. Stumm and Morgan (1970) reviewed the problem and
concluded that while soluble organic complexes of iron in
natural waters could not be discounted entirely, it is more
probable that insoluble organic-hydroxy-iron species are
present in stable colloidal dispersion.

Sholkovitz (1976) performed an elegant series of
experiments on the chemical composition of the precipitates
formed when filtered Scottish river waters were mixed with
filtered seawater under a variety of conditions. The amount
of precipitated material per liter of river water in the
mixture increased with increasing salinity; Fe, Mn, Al, P,

Table 1. Recent work on a) iron-organic association, and
        b) colloidal properties of iron oxide.

Reference

a) Shapiro (1958)   Chromatography of organic-iron
                                complexes from lake water

    Hem (1960)   Complexes of ferrous iron with
                                tannic acid

    Schnitzer and Skinner   Properties of soil organic matter-
    (1963a)   cation complexes

    Schnitzer and Skinner   Reaction between soil organic mat-
    (1963b)   ter and iron and aluminum oxides

    Schnitzer and Skinner   Reaction between soil organic
    (1965)   matter and cation-saturated
                                ion-exchange resins

    Levesque and Schnitzer   Fulvic acid - metal phosphates
    (1967)

    Ong and Bisque (1968)   Coagulation of humic colloids
                                by metal ions

    Khan (1969)   Acid-base titrations of humic
                                acid - metal cation mixtures

    Martin, Doig, and Pierce   Correlation of iron and humic
    (1971)   acid in Florida streams

    Rashid (1971)   Complexing of cations by marine
                                humic acids

    Theis and Singer (1974)   Complexation of Fe(II) by tannic
                                acid and effect of organics on
                                Fe(II) oxidation kinetics

    Beck, Reuter, and Perdue   Distribution of organic and
    (1974)   inorganic constituents in Georgia
                                coastal plain rivers

b) Deb (1949)   Colloid-stabilizing effect of
                                soil organic matter on iron
                                oxide sols

    Schnitzer and Delong   Electrodialysis of leaf extracts
    (1955)   enriched with iron

Lengweiler, Buser, and Feitknect (1961)	Ultracentrifugation of "soluble" iron oxide colloids
Shapiro (1964)	Chemistry of yellow organic matter isolated from lake water and its stabilizing effect on iron colloids
Lamar (1968)	Chemistry of organic matter isolated from stream water; removal of natural iron colloids from stream water by ultrafiltration
Perhac (1972)	Distribution of elements on particulate, colloidal, and dissolved fractions in Tennessee streams
Kennedy, Zellweger, and Jones (1974)	Filter pore size effects on the analysis of Fe, Al, Mn, and Ti in freshwater samples

and organic carbon all behaved similarly. The reaction was observed to be rapid with most of the precipitate forming within 1/2 hr. Eckert and Sholkovitz (1976) studied the effect of various salts on the precipitation. They found that the amount of precipitate increased in the sequence $NaCl<<MgCl_2 < CaCl_2$. These results were interpreted in terms of cation-induced coagulation of humic colloids containing bound iron and other elements. This series of experiments established a definite association between iron and organic matter and provided important information about the mechanism of iron removal in estuaries.

The present investigation was undertaken to examine the freshwater and estuarine geochemistry of iron to establish its chemical form and understand its reactivity.

Methods

In the summer and fall of 1973 a number of east coast U.S. estuaries were surveyed to determine whether iron removal processes are widespread.

Surface water samples were collected throughout the salinity range (for example, see fig. 1) and immediately filtered through acid-leached glass fiber filters. Within 24 hours after collection the samples were acidified to pH=2 with hydrochloric acid. For the 10/13/74 Mullica estuary samples a Whatman GF/F glass fiber filter (nominal pore size 0.7µm) was used; for the rest of the samples Mead glass fiber filters (nominal pore size 1.2µm) were used. Glass fiber filters were chosen over membrane

filters because their greater flow velocity allows for
immediate filtration of turbid estuarine waters and avoids
the storage effects noted by Lewin and Chen (1973). This
advantage comes at the cost of precise pore size definition,
a problem which will be discussed later.

Salinity was determined on an unacidified split by
conductivity, chloride selective electrode, or chloride titration
using a Buchler/Cotlove chloridometer. The iron content of the
samples was determined colorimetrically following reduction by
hydroxylamine for one hour at room temperature. An acetate
buffer was used with bipyridyl or ferrozine (Stookey, 1970)
as the color forming reagent. A water color blank correction
was measured for each sample. Only that fraction of iron
originally present as Fe^{2+} (aq) or converted to Fe^{2+} by the
reduction procedure is determined by this method, referred
to in the text as "colorimetric iron". The precision of
the determination is approximately ± 0.1 µmol/l or $\pm 3\%$,
whichever is greater.

Organic matter interferes with the determination of
ferrous iron in natural water samples by reducing ferric iron
(Shapiro, 1966; McMahon, 1967). An upper limit for Fe^{2+} (aq)
was estimated by immediate colorimetric analysis of filtered
samples at intermediate pH with the elimination of the
reducing reagent.

Total iron was determined by direct injection heated
graphite atomizer atomic absorption spectrophotometry (Segar
and Cantillo, 1975) using an internal additon on each sample

for standardization. The estimated precision of this analysis
is ± 0.05 μmol/l or $\pm 5\%$, whichever is greater. A Perkin-Elmer
HGA-2100 graphite furnace and model 403 spectrophotometer with
model 56 chart recorder were used for the analyses.

Analysis of precipitates formed in the mixing experiments
described in the test was by thin-film X-ray fluorescence and
chromatography using a CHN elemental analyzer (Sholkovitz, 1976).
To elucidate the chemical form of iron and the naturally-
occurring processes, various filtration experiments were
performed as discussed in the text using 0.45μ, 0.10μ in
0.05μ Millipore membrane filters.

Results and discussion

1) Field results

Data from the east coast United States estuaries
(Table 2) are displayed in plots of iron vs. salinity in
Fig. 1. All of the estuaries studied show negative curvature
from a two end-member iron-salinity mixing line and demonstrate
that iron is removed from solution in the mixing zone. None
of the estuaries studied have significant tributaries in the
mixing zone. Lower limits on the degree of removal were
calculated using the flux model of Boyle et al. (1974) (Table 3).
Removal of iron ranges from 50% to greater than 95% among the
rivers studied. The iron concentration of the river end
member varies from 3 to 24μmol/ ; rivers of higher iron
concentration have a greater total removal in their estuaries.
This iron removal process has been observed now in at least
eight estuaries on fourteen occasions and is therefore

Table 2. Iron and Salinity Data for Some East Coast United States Estuaries.

(1)		(2)		(3)		(4)		(5)	
S	Fe	S	Fe	S	Fe	S	Fe	S	Fe
0.06	8.5	0.05	4.0	0.29	0.3	0.07	3.5	0.38	11.9
0.08	1.1	0.05	4.0	0.38	1.0	0.38	3.3	0.44	12.5
0.45	8.5	1.3	3.1	2.1	0.0	2.1	3.2	1.05	12.5
2.1	5.5	5.3	2.5	4.1	0.3	4.8	2.5	2.88	11.5
2.5	3.6	5.3	2.3	6.9	0.0	7.3	1.6	3.73	6.6
12.5	1.2	14.4	1.2	9.9	0.0	10.4	1.5	5.76	5.8
12.5	0.8	20.6	0.8	10.9	0.1	13.1	4.0	7.61	4.8
		25.6	0.7	12.6	0.4	15.8	0.8	11.59	3.0
		25.6	0.6	19.4	0.0	17.6	0.8	16.61	2.5
		27.5	0.1	23.8	0.3	21.9	1.0	20.60	1.9
				23.8	0.3	27.5	0.5	26.76	1.3
				31.3	0.2	33.8	1.0	27.94	1.0

(6)			(7)		
S	Fe	Fet	S	Fec	Fet
0.26	3.3	11.0	0.25	23.4	24.9
0.30	3.0	16.4	0.31	22.9	28.7
0.56	4.1	13.3	0.83	18.8	20.4
1.23	1.8	6.5	1.70	14.6	16.7
2.47	0.5	1.5	2.54	10.9	16.4
2.56	0.6	1.8	3.82	8.0	9.2
2.93	0.5	2.2	4.06	8.0	10.0
3.19	0.2	0.64	8.57	3.4	3.4
3.20	0.3	1.4	9.81	2.4	2.5
8.97	0.1	0.28	11.73	1.9	1.9
10.47	0.1	0.23	13.32	1.4	1.8
13.85	0.1	0.23	15.84	1.1	1.4
			20.13	0.7	
			21.89	0.6	
			22.12	0.6	
			22.51	0.5	
			23.82	0.5	
			25.34	0.9	
			25.73	0.4	
			29.03	0.4	

Table 2 (Cont'd)

(8)

S	Fe
0.16	3.07
0.16	3.08
0.17	2.94
0.17	2.56
0.31	2.71
1.19	2.67
1.39	2.67
2.04	2.43
2.52	2.30
2.90	2.09
3.06	2.23
3.70	2.03
4.26	2.02
4.37	1.94
5.78	1.62
10.43	1.00
10.66	0.68
13.12	0.37
15.27	0.68
15.98	0.70
18.41	0.52
23.48	0.26
29.34	0.07
30.46	0.05

(9)

S	Fec	Fet	pH
0.09	3.59	4.86	6.5
0.17	4.22	5.75	6.5
0.58	4.91	6.92	6.4
0.93	5.18	8.29	
1.18	6.05	9.27	6.6
1.82	5.00	7.06	
2.32	4.35	6.80	6.7
3.04	4.43	6.65	
4.22	3.73		6.9
4.42	3.48	5.21	
5.76	3.05		6.9
7.45	2.91	4.20	
8.53	2.74		
10.48	2.31		7.1
11.79	1.89	2.52	
13.43	1.73		7.2
14.86	1.32		
15.84	1.28	1.75	7.4
17.48	1.25		7.5
20.61	1.11		
21.86	0.95		
23.31	0.75		
25.31	0.57	0.90	
27.33	0.58		
27.55	0.51		

Table 2 (cont'd)

(1) Connecticut Estuary, Conn., 7/5/73, B-12 (*).
(2) Merrimack Estuary, Mass, 7/26/73, B-5.
(3) Connecticut Estuary, Conn., 8/10/73, B-7.
(4) Merrimack Estuary, Mass., 8/14/73, B-3.
(5) Parker Estuary, Mass., 8/21/73, B-26.
(6) Rappahannock Estuary, Virginia, 9/3/73, B-22.
(7) Mullica Estuary, New Jersey, F-153.
(8) Connecticut Estuary, Conn., 11/11/73, F-3.
(9) Parker Estuary, Mass., 10/14/74, F-5
(10) Merrimack Estuary, 10/30/73, F-8. See Boyle et. al. (1974).

* Analytical code: B= bipyridyl reagent, F= ferrozine reagent; followed by number of days between acidification and analysis.

S = salinity, o/oo

Fe_c = colorimetric iron, $\mu mol/l$

Fe_t = total iron, $\mu mol/l$

Figure 3-1. Iron vs. salinity data from preliminary

survey of east coast U.S. estuaries.
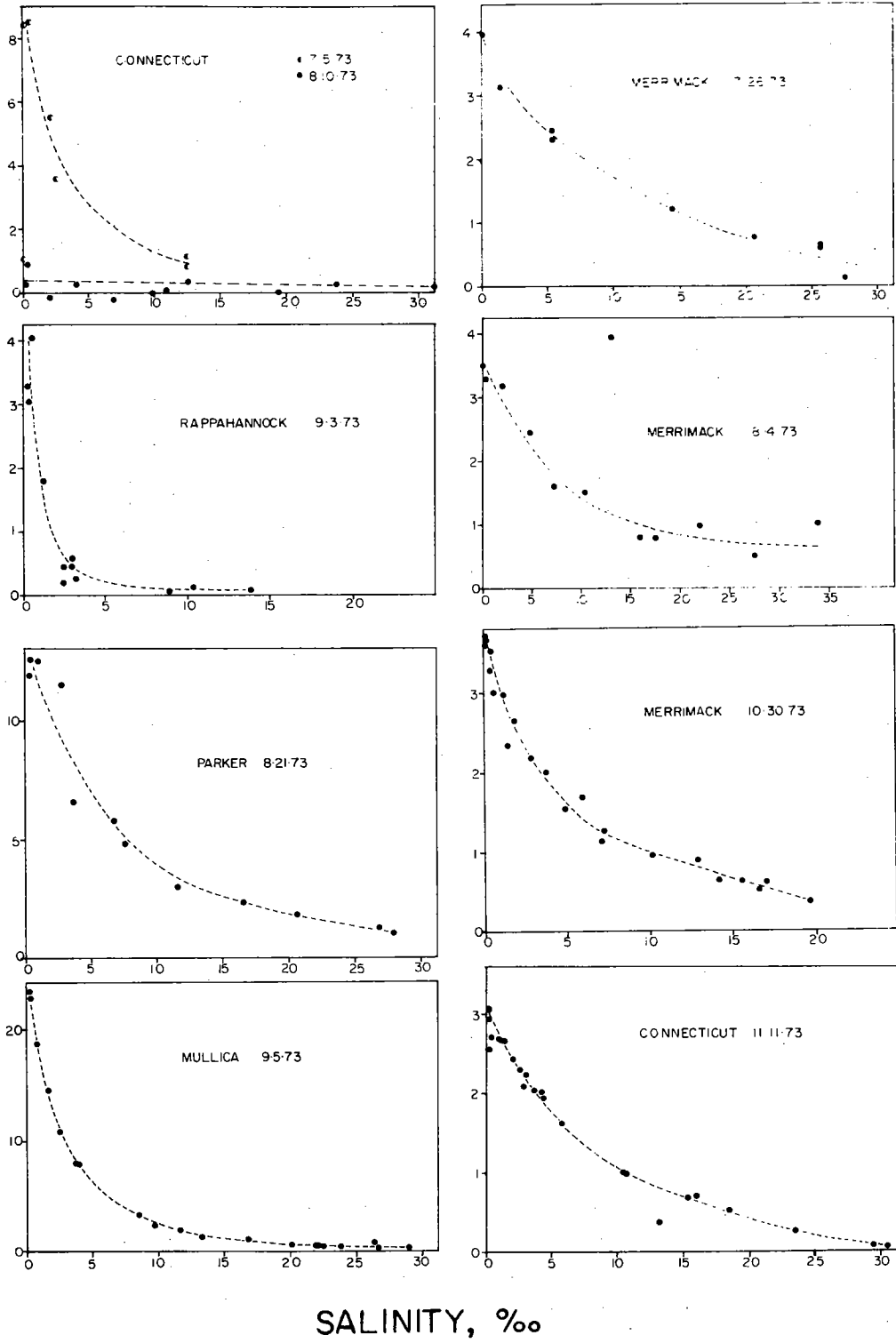
Table 3. Iron removal from some east coast estuaries.

Estuary	Zero-salinity end member Iron, μmol/l	High-salinity Intercept Iron, μmol/l	% Removal
Connecticut 7/5/73	8.5	2.5	71
11/11/73	3.1	0.9	71
Merrimack 7/26/73	4.0	1.5	63
8/14/73	3.5	1.0	71
10/30/73	3.7	1.7	54
Parker 8/21/73	11.9	4.0	66
Mullica 9/5/73	23.4	1.0	96
Rappahannock 9/3/73	3.3	0.3	91

established as a common phenomenon.

The iron concentrations plotted in Fig. 1 are based on the colorimetric method described earlier. This method will determine only that fraction of the iron converted to Fe^{2+} by the relatively mild conditions employed. The possibility that some fraction of the iron in the filtered solution is not determined by this analysis must be considered. Analyses for total iron by the flameless atomic absorption method are plotted vs. colorimetric analyses in Fig. 2. For two of the estuaries the total iron concentrations are significantly higher than the colorimetric analyses. The ratio of the concentrations as determined by the two methods is almost constant for a given estuary; a plot of total iron vs. salinity displays the same negative curvature as the plots shown in Fig. 1. Total iron is also removed from solution in these estuaries. One of the samples from the 10/13/75 Mullica estuary trip gave considerably more total iron than colorimetric iron. It was therefore re-analyzed in duplicate both by the colorimetric method and by a modification in which the sample was boiled for 1/2 hour after additon of hydroxylamine. This procedure increased the colorimetric analysis to near the level observed for total iron. Some fraction of the total iron is converted to Fe^{2+} only by the harsher conditions. An explanation for the iron removal phenomenon should account for these analytical differences and will be discussed later.

2) Preliminary mixing experiment

Laboratory mixing experiments were performed to constrain

Figure 3-2. Total iron vs. colorimetric iron for

estuarine samples.
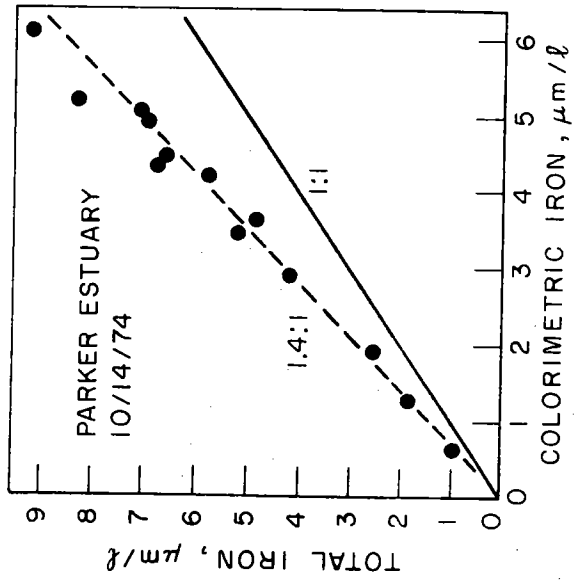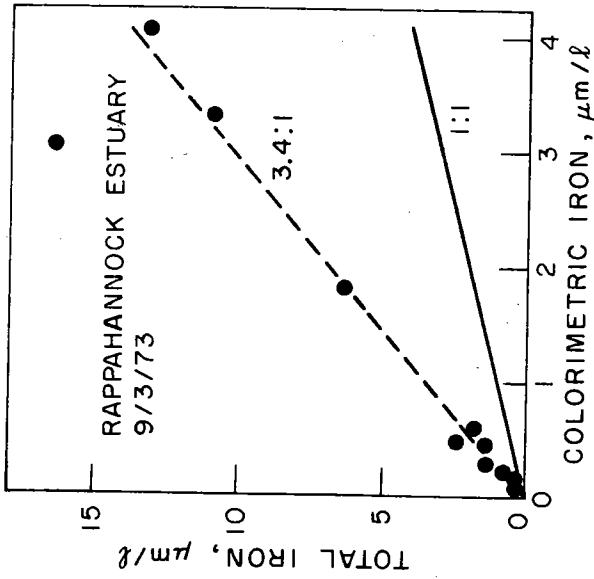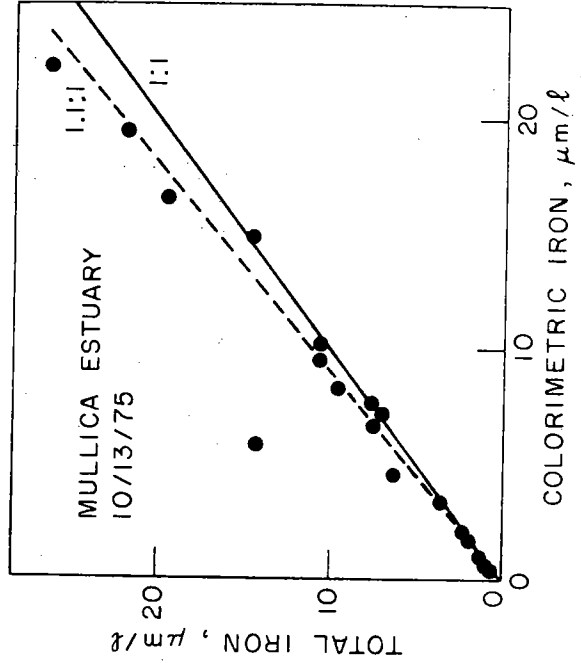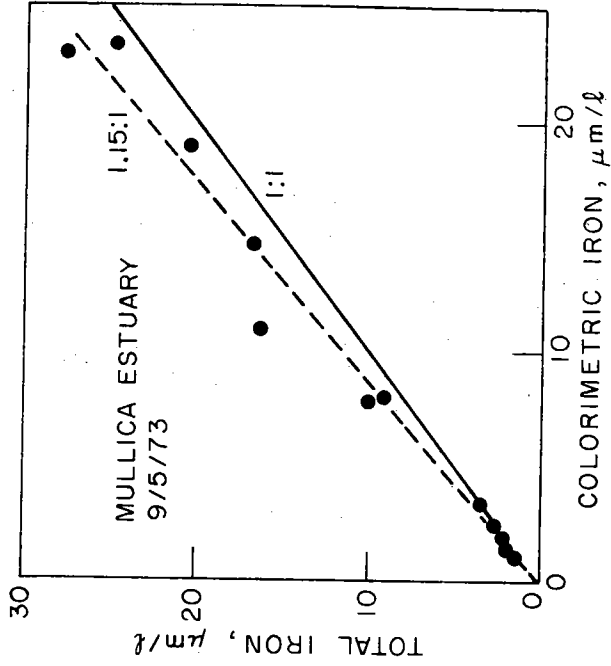
the factors controlling the removal of iron when fresh
and saline waters meet. Water was taken from the Merrimack
River at Lowell, Mass. (3/6/74). Unfiltered and Mead-glass-
fiber-filtered aliquots were mixed with equal volumes of
(1) distilled water, (2) 0.7 N NaCl, (3) seawater diluted
to 10% salinity, (4) seawater, and (5) seawater acidified with
hydrochloric acid to pH=6.5. Each of these mixtures was
allowed to stand for 3 hours and 24 hours before being
refiltered through a Mead glass fiber filter. Iron analyses
were then performed using the room-temperature reduction
colorimetric method previously described (Table 4). The
reaction is rapid, with little additional removal occurring
after 3 hours. The removal percentage depends on the salinity
of the mixture, with less removal taking place at lower
salinity. The effect is not simply related to ionic strength,
since 0.7 M sodium chloride solution is less effective than
seawater. Evidently there is a specific interaction with
seawater species other than sodium or chloride ions, in
agreement with the results of Eckert and Sholkowitz (1976).
Changes in solution pH over the range of values likely to
be encountered in estuaries do not strongly affect the
precipitation: seawater acidified to pH=6.5 (the same pH
as the river water) is only slightly less effective. The
results demonstrate that presence of river-borne particulate
matter also has only a minor effect on the extent of precipit-
ation. Precipitation of iron in estuaries is controlled
by an effect related to the specific ionic composition of

Table 4. Initial Mixing Experiments.

Mixing Solution	Filtered or unfiltered	Mixing Time, hr.	% Removal*
Distilled water	F	4	11
	F	24	8
	U	4	16
	U	24	12
10 ‰ seawater	F	4	27
	F	24	32
	U	4	38
	U	24	40
30‰ seawater, pH=8.2	F	4	60
	F	24	66
	U	4	72
	U	24	78
30‰ seawater, pH=6.5	F	4	53
	F	24	58
	U	4	48
	U	24	42
0.7 M NaCl	F	4	21
	F	24	26
	U	4	25
	U	24	25

*Iron determined colorimetricly using ferrozine 4 days after acidification. Measured iron concentration in the initial filtered river water was 3.36 μmole/liter.

seawater.

3) The role of ferrous iron

The possible role of ferrous iron in the estuarine removal process was considered. At low pH values the oxidation rate is slow enough to give Fe^{2+} a half-life of days to weeks (Stumm and Lee, 1961); when a low-pH river mixes with higher-pH seawater, Fe^{2+} should oxidize and precipitate as hydrated ferric oxide. Gjessing (1964) reported that a high percentage of the total iron in some Norwegian freshwater samples was in the ferrous state. But Shapiro (1966) and McMahon (1967) demonstrated that this observation of ferrous iron was an artifact of the analytical procedure: under acidic conditions natural organic matter will reduce ferric iron, the reaction being accelerated by heat and bright light. An upper limit for ferrous iron can be estimated by immediate colorimetric analysis at intermediate pH. This method was used in two of the estuaries studied (Parker, 10/30/74 and Mullica, 10/13/74) and indicated that ferrous iron comprised less than 10% of the total iron. The absence of a pronounced pH effect, as shown in the mixing experiments mentioned earlier, also suggests that oxidation of ferrous iron is not a significant mechanism for iron removal in estuaries.

4) The mechanism of iron removal

A combined field and laboratory study of the Mullica estuary was undertaken to study in detail the mechanism of iron precipitation. This estuary was chosen because iron removal previously was observed as extensive(>95%).

a) Field Data

The field data for total iron and salinity (Table 5, Fig. 3) demonstrate that iron removal was occurring in the Mullica estuary as previously observed.

b) Mixing Experiments

The laboratory mixing experiments were performed on river water prefiltered successively through a Mead glass fiber filter, a Whatman GF/F glass fiber filter, and twice through an 0.45μm Millipore membrane filter. The procedure was modeled after that of Sholkovitz (1976). Three filter types were used for the purposes of different analyses. The filtered river water was mixed in varying proportions with filtered seawater and NaCl, $MgCl_2$, and $CaCl_2$ solutions. Each mixture was then processed as described by the flow chart in figure 4. The combined filtrates (both 1 hr. and 1 day) were analyzed for total iron. Fe, P, Al, Ti, and Si determinations were performed on the Millipore filters; particulate organic carbon was determined on the glass fiber filter. The preweighed Nuclepore filters were washed with small portions of distilled water, dried in a dessicator and reweighed. The low ionic strength of the wash solution tends to peptize the precipitate, but the disaggregation is slow compared to the rinse time and little net weight is lost. The results of these analyses are listed in Table 6.

The laboratory mixing experiments (Table 6, Fig. 5) mirror the field observations. The differences in absolute

Table 5. Data from the Mullica Estuary, 10/13/75

Salinity ‰	Total Iron μmol/l	LT Color. Iron μmol/l **	HT Color. Iron μmol/l **	pH
0.00	9.5*	8.3		
0.00	7.1*	7.4		
0.22	25.4	22.4	22.4	
0.90	21.9	19.7	19.4	
1.61	14.1	5.8	12.2	
		6.1	12.8	
2.20	18.7	16.6	16.5	
3.23	14.6	14.9		
5.27	10.6	10.1		
5.60	10.6	9.6	9.6	
7.13	7.6	6.7		
9.09	6.3	4.6		
9.61	3.6	3.3	3.3	
12.07	2.1	2.0		
12.29	2.2	2.0	2.0	
13.84	1.7	1.6	1.5	7.6
16.27	1.1	1.0		7.6
18.54	0.9	0.6		7.7
21.17	0.3	0.3		7.8
22.66	0.2	0.3		7.9
24.59	0.2	0.2	0.2	7.9
27.38	0.1	0.0		8.0
28.44	0.1	0.0		8.0
29.77	0.0	0.0		8.1
30.34	0.0	0.1		8.2

*These samples were allowed a long filtration time through a highly clogged filter; reduction of the pore size by the clogging is the most likely explanation for these low values, as discussed in the conclusion.

**Colorimetric analyses using ferrozine 93 days after acidification.
LT = room temperature reduction with hydroxylamine (1 hr.)
HT = boiling reduction with hydroxylamine (1/2 hr.)

Figure 3-3.   Total Iron vs. salinity, Mullica Estuary,

10/13/75.

MULLICA ESTUARY 10/13/75
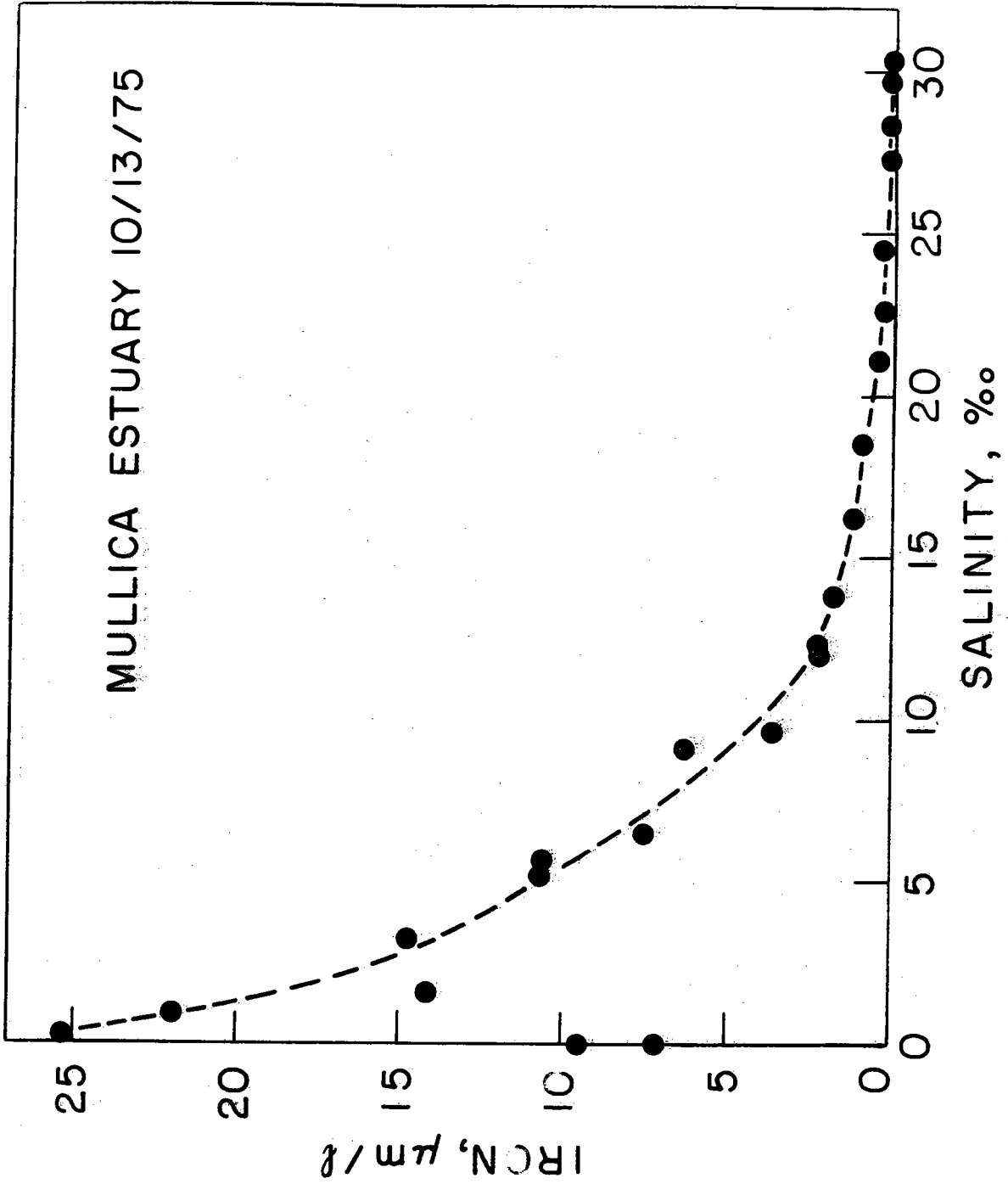
Figure 3-4.   Flow chart describing mixing experiments

with filtered Mullica River water.

```
┌──────────┐                    ┌──────────┐
│ FILTERED │                    │ FILTERED │
│  RIVER   │                    │   SEA    │
│  WATER   │                    │  WATER   │
└──────────┘                    └──────────┘
```

MIX. STAND 1 HOUR

```
┌────────────────┐  ┌────────────────┐  ┌────────────────┐
│ FILTER THROUGH │  │ FILTER THROUGH │  │ FILTER THROUGH │
│ 0.45µ MILLIPORE│  │ 0.4µ NUCLEPORE │  │ WHATMAN GF/F   │
│    FILTER      │  │    FILTER      │  │ GLASS FIBER    │
│                │  │                │  │    FILTER*     │
└────────────────┘  └────────────────┘  └────────────────┘
```

COMBINE FILTRATES
STAND 1 DAY

```
┌────────────────┐  ┌────────────────┐  ┌────────────────┐
│ FILTER THROUGH │  │ FILTER THROUGH │  │ FILTER THROUGH │
│ 0.45µ MILLIPORE│  │ 0.4µ NUCLEPORE │  │ WHATMAN GF/F   │
│    FILTER      │  │    FILTER      │  │ GLASS FIBER    │
│                │  │                │  │    FILTER*     │
└────────────────┘  └────────────────┘  └────────────────┘
```
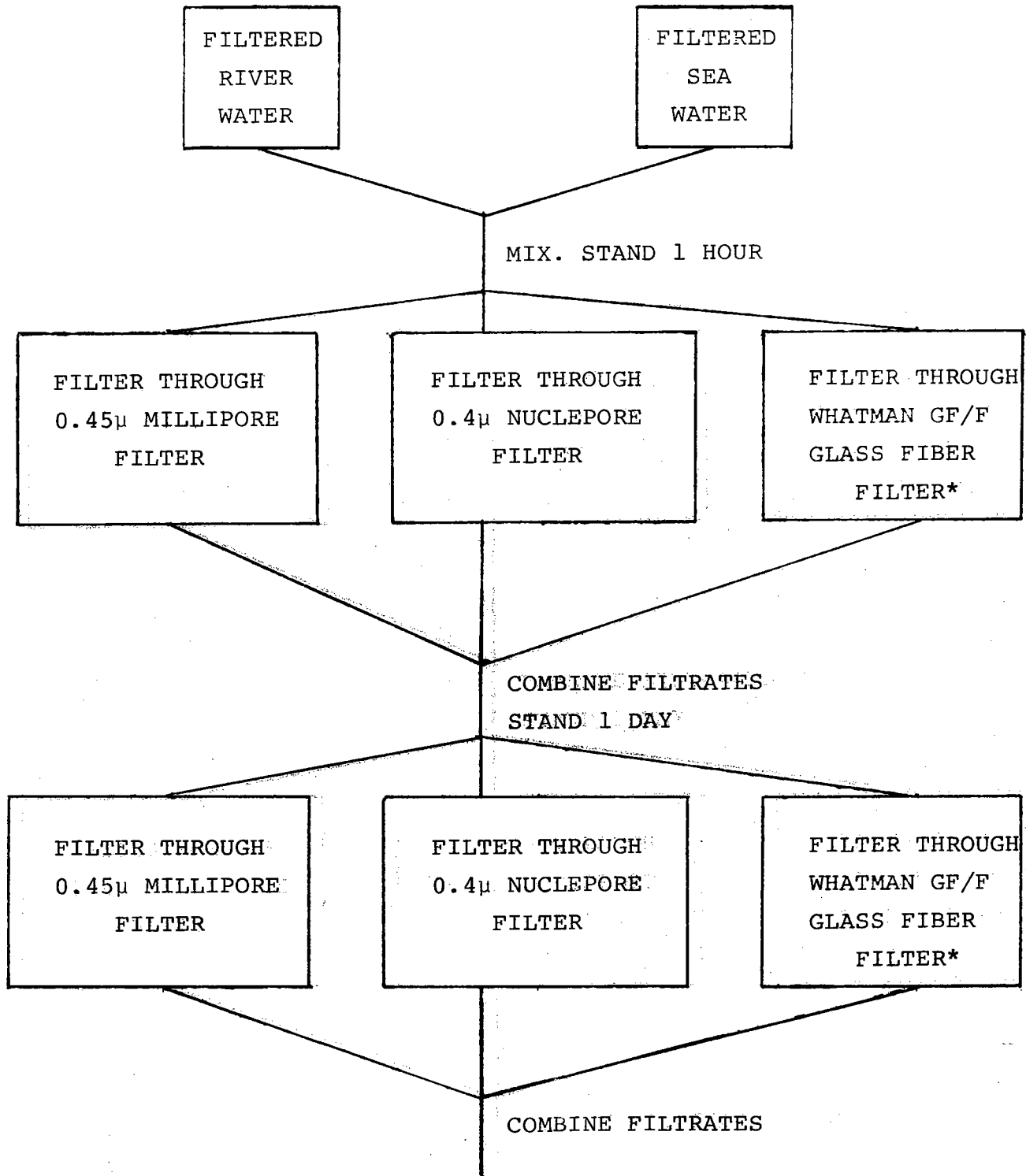
COMBINE FILTRATES

* PRECOMBUSTED

NOTE: equal portions (±10%) were filtered through each filter

Table 6. Mixing experiments using filtered Mullica River Water.

Salinity of mixture ‰	FILTRATE Total Iron µmol/l of mixture	PARTICULATES µg/liter of river water**						
		Total Weight	Fe	P	Al	Ti	Si	Organic carbon
0	15.5	---	0*	0.0*	0.0*	0.00*	0*	0*
2	13.9	150	145	1.5	3.6	0.38	0	0
5	8.3	---	367	4.5	9.9	0.69	5	0
9	4.2	1602	414	7.6	13.4	0.13	12	287
14	0.63	3185	1016	21.	33.1	0.52	86	564
18	0.28	2982	1044	27.	31.2	0.30	68	129
28	0.11	2121	1041	67.	44.0	0.00	0	328

1 hr.

Salinity of mixture ‰	FILTRATE Total Iron µmol/l of mixture	PARTICULATES µg/liter of river water**						
		Total Weight	Fe	P	Al	Ti	Si	Organic carbon
0	16.0	---	0*	0.0*	0.0*	0.00*	0*	0*
2	11.8	---	98	0.5	0.0	0.85	11	0
5	8.2	---	247	3.7	2.7	0.26	27	0
9	2.0	853	381	13.	11.0	0.05	41	0
14	0.57	140	35	14.	0.7	0.42	10	0
18	0.21	317	3	15.	4.2	0.00	13	415
28	0.06	847	0	36.	10.0	0.00	41	0

1 day

|	FILTRATE Total Iron µmol/l of mixture	PARTICULATES µg/liter of river water**						
3.2x10⁻³ M 1 hr	5.11	---	200	3.2	4.4	0.22	59	---
CaCl₂ 24 hr	--	---	53	3.2	3.6	0.15	3	---
1.6x10⁻² M 1 hr	3.36	---	680	13.0	31.2	0.52	92	---
MgCl₂ 24 hr	--	---	6	4.7	0.0	0.18	7	---
1.6x10⁻¹ M 1 hr	5.74	---	430	3.0	6.3	0.49	97	---
NaCl 24 hr	--	---	49	0.3	0.0	0.03	1	---

*Zero-salinity particulate "blank" subtracted from the listed values (Sholkovitz, 1976). Hence the zero salinity results are zero by definition.

**Total on filters divided by the volume of river water in the filtered mixture.

Figure 3-5. Total iron vs. salinity, Mullica River

water mixing experiments.
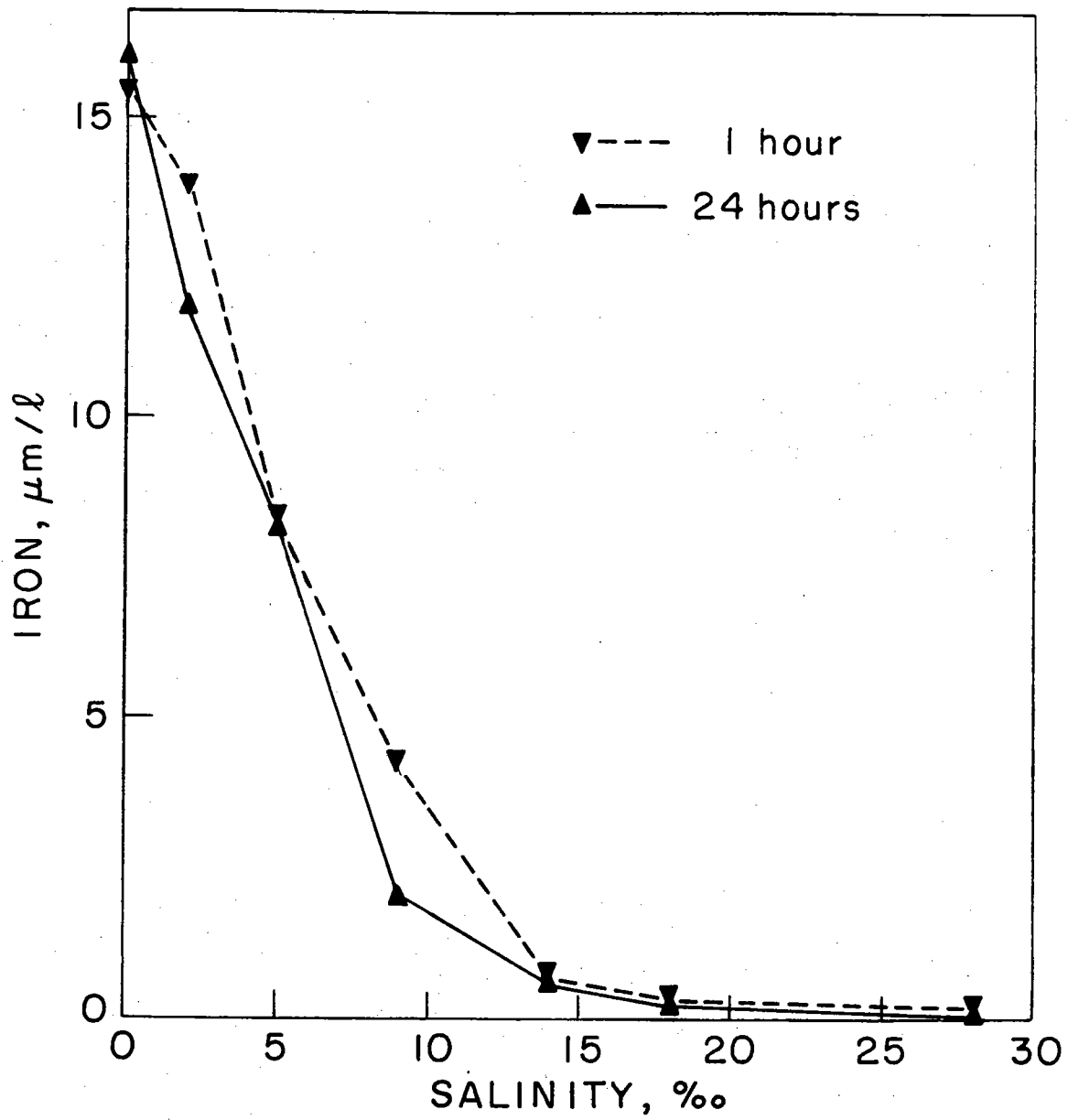
concentration reflect the different filtration procedures employed, a point that will be discussed later. As observed by Sholkovitz, the precipitation is cation-dependent. Solutions of major seawater salts were added individually to the river water up to levels equivalent to their concentration in 10‰ estuarine water. At these concentration levels, magnesium is more effective than calcium and sodium (Table 6).

The kinetics of the precipitation reaction were studied by filtering three different seawater-filtered river water mixtures (salinities of the mixtures were 5‰, 9‰, and 14‰) at known time intervals through an 0.45μ filter. The reaction is extremely rapid (Table 7, Fig. 6) with a time scale of a few minutes. The iron concentration decreases to an apparent "equilibrium" level characteristic of the salinity of the mixture.

The chemical composition of the particulates follows patterns similar to those observed by Sholkovitz (1976). Organic matter and iron are the major components of the precipitate. Phosphorous, manganese. and aluminum are also incorporated into the precipitates. Silicon is precipitated, but the total amount is small relative to the river concentration of dissolved silicon (100μmol/l). These results confirm and extend the conclusions discussed earlier and those of Sholkovitz (1976).

c) Precipitate Redissolution

In view of the apparent salinity-dependent "equilibrium" iron concentrations observed in the mixing experiments, the

Table 7. Kinetics of Precipitation.

5 o/oo		9 o/oo		14 o/oo	
time,min	total iron μmol/l	time,min	total iron μmol/l	time,min	total iron μmol/l
0	10.6*	0	9.3*	0	7.9*
0.4	7.5	0.3	5.4	0.3	2.8
1.0	6.4	0.7	4.8	0.7	2.6
1.5	6.6	1.0	5.1	0.9	2.6
2.3	7.0	1.3	4.8	1.2	1.8
3.2	5.6	1.6	4.3	1.6	2.0
4.6	5.8	2.2	4.5	2.0	1.9
6.1	5.8	2.7	4.4	2.7	1.6
8.3	5.6	3.5	4.2	3.5	1.4
9.7	4.9	4.8	3.9	4.9	1.1
12.4	5.2	6.8	4.2	6.4	0.7
15.1	4.9	10.2	2.8	9.7	0.7
19.5	3.9	15.3	2.5	15.5	0.6
25.1	3.9	20.2	2.1	20.7	0.7
36.2	3.8	29.7	2.0	30.4	0.6
48.6	3.7	40.1	1.8	41.9	0.7
68.0	3.6	93.3	1.6	62.2	0.6

*t=0 iron concentration measured on the unfiltered mixture.

Figure 3-6. Kinetics of precipitation of iron from

filtered Mullica River water - seawater

mixtures.
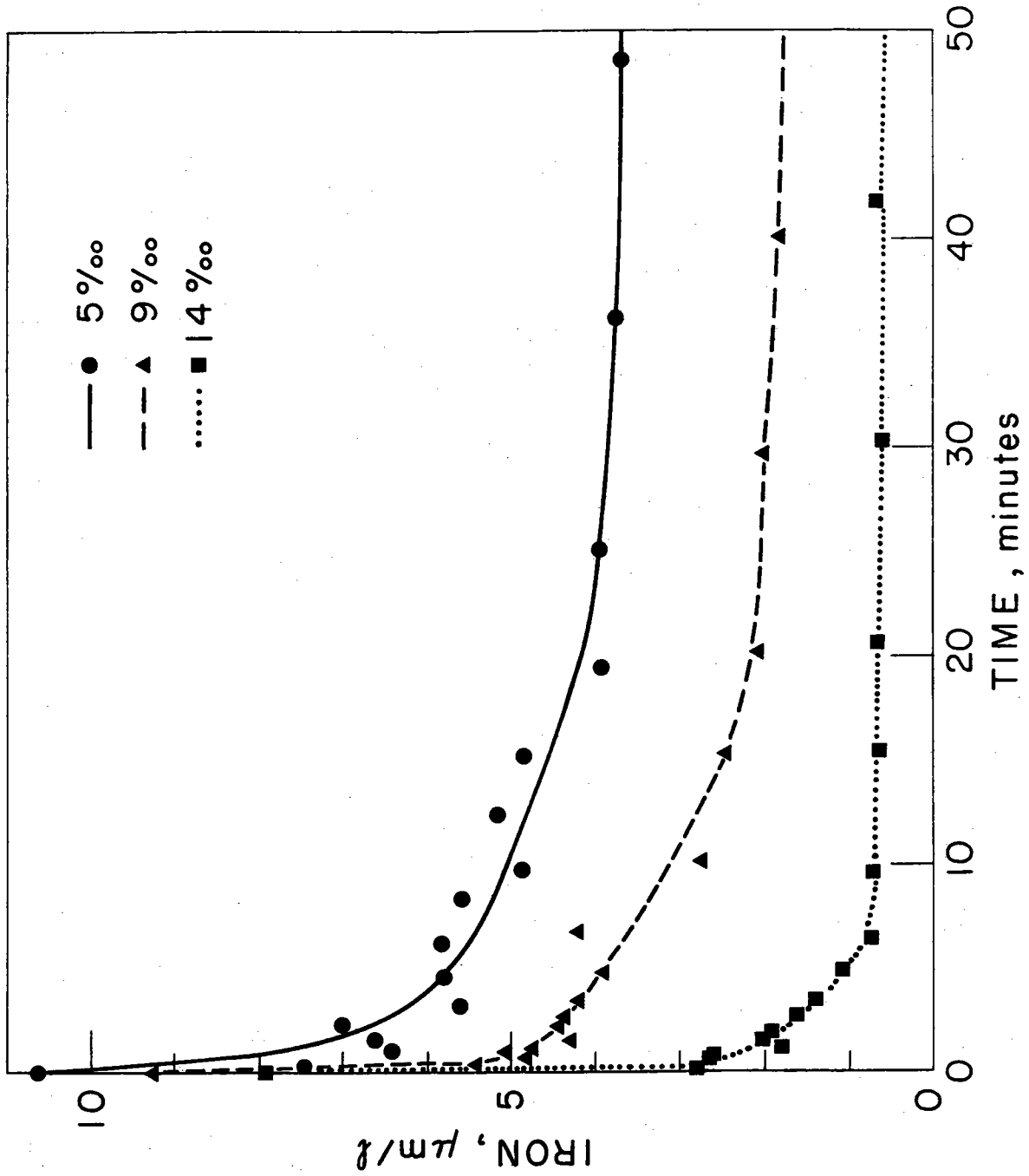
redissolution behavior of the precipitate was studied. A large quantity of precipitate was collected by adding $CaCl_2$ to the filtered river water (0.1 M), centrifuging and briefly washing the excess $CaCl_2$ from the precipitate with distilled water. Samples of this precipitate were mixed with various seawater/distilled water mixtures, dispersed in an ultrasonic bath for 15 minutes and then filtered through an 0.45μ Millipore filter after standing for 1, 2, and 9 days. The filtrates were analyzed for total iron. The form of the Fe-S curves (Fig. 7) is similar to those observed for the precipitation process, but lower iron concentration levels are observed which change with time. Although the precipitation resembles an equilibrium process, strictly the reaction is not completely reversible.

d) Cation Effect

The effect of different cations on iron precipitation provides clues to the nature of the cation-organic inter-action. For this experiment small portions of concentrated chloride or sulfate salts of Mn, Co, Ni, Cu, Zn, Mg, Ca, Sr, and Ba were added to filtered river water. The mixture was allowed to stand for 45 min., and then was refiltered through an 0.45μ filter and the filtrate analyzed for total iron. The experiment was performed initially at final cation concentrations of 3×10^{-3}M. From these results an estimate was made for the individual cation concentrations required to precipitate equal quantities of iron. The experiment was then redone at these new concentration levels; the results of this second iteration

Figure 3-7. Redissolution experiment: total iron

vs. salinity.
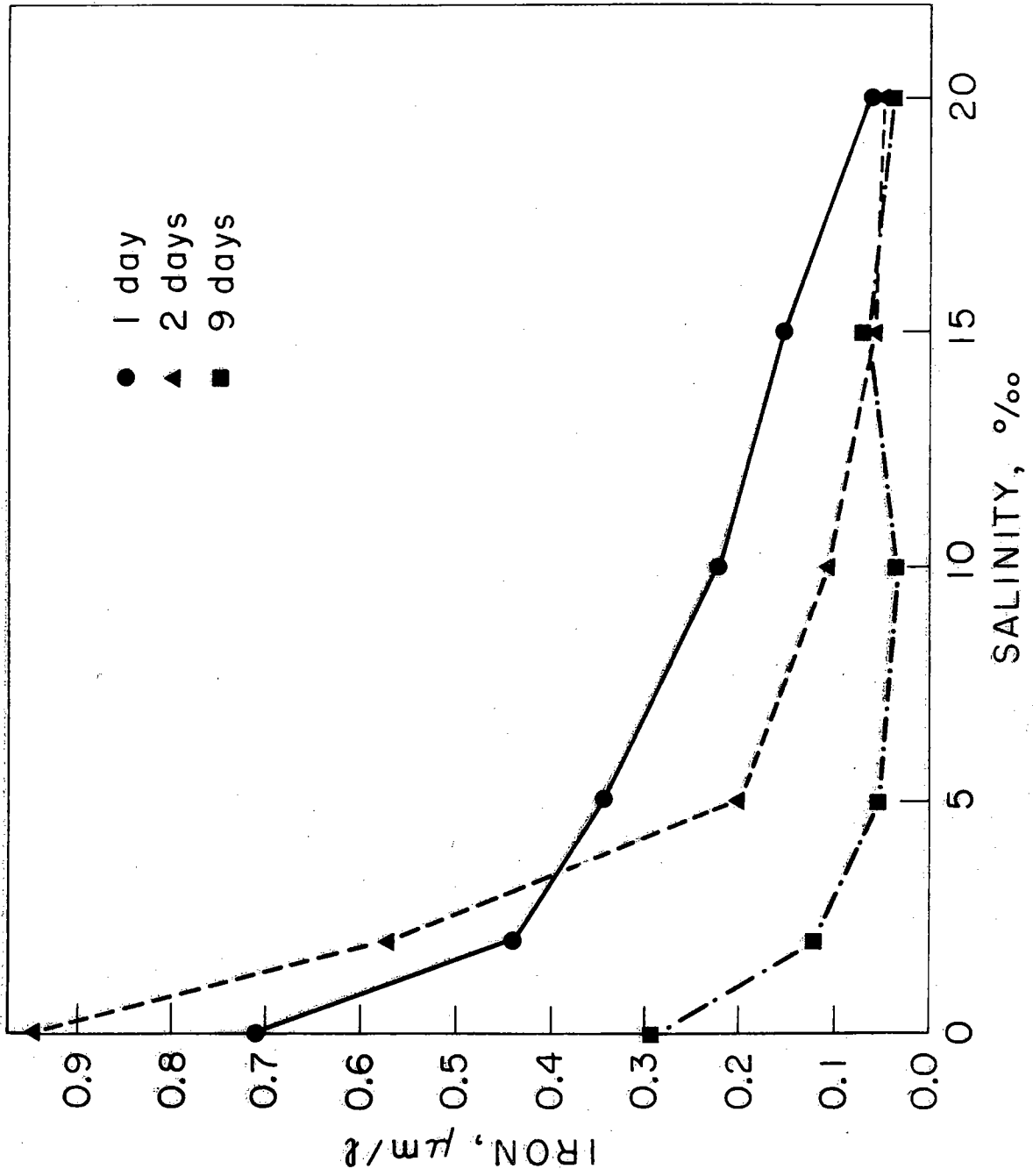
are given in Table 8. The divalent first row transition

metals are increasingly effective in the sequence

Zn<Mn<Co∿Ni<<Cu. This order demonstrates that there is a

specific chemical interaction between the metal ion and the

organic matter in addition to purely electrostatic effects,

as has been observed for the stability constants of 1:1

complexes of these metals (Irving and Williams, 1953).

The alkaline earth metals display the order Mg<Ca<Sr<Ba.

This order is unlike the stability sequence observed for

most chelating agents (Phillips and Williams, 1966) but

is similar to that observed for large strong-acid anions

(Phillips and Williams, 1966) and many ion-exchange

materials (Stumm and Morgan, 1970).

e) Colloidal nature of iron in river water

Iron alone accounts for at least 25% of the total

weight of the precipitate formed during the mixing of

river water with seawater. This high percentage of iron

makes it highly unlikely that the precipitate is a simple

organic-iron complex. If all of the remaining 75% of the

precipitate was organic matter forming a 1:1 complex with

iron, the average molecular weight of the organic material

would be 170. This is an extreme upper limit, as other

components are present in the precipitate. Most evidence

suggests that the molecular weight of freshwater organic

matter is no lower than 400 (Shapiro, 1958).

On the other hand Deb (1949) demonstrated that humic

materials can stabilize colloidal iron oxide at iron/carbon

Table 3.   The effect of various cations on iron precipitation.

Salt	Concentration, $\mu mol/l$	Total iron*, $\mu mol/l$
$MgCl_2$	7.3	6.4
$CaCl_2$	3.3	7.8
$SrCl_2$	2.7	5.8
$BaCl_2$	1.7	5.7
$MnCl_2$	2.7	6.5
$CoCl_2$	2.0	6.4
$NiSO_4$	2.0	6.5
$CuSO_4$	1.3	3.1
$ZnSO_4$	2.7	7.6

*The initial iron concentration of the river water was 12.3 $\mu mol/l$; the dilution due to addition of the cation solutions was < 0.6%.

atom ratios as high as 4. This type of "solubili-
zation" mechanism is more compatible with the high iron
content of the precipitate. To test directly for the
presence of colloidal iron, Mullica river water was
filtered through an 0.45μ filter and subjected to ultra-
centrifugation and to refiltration through 0.10μ and
0.05μ filters (Table 9). Filtration through filters of
successively smaller pore size removed an increasing
amount of iron, up to 79% at 0.05μ . Increasingly severe
ultracentrifugation sedimented up to 76% of the iron
(90,000 g, 3 hr.); a brown pellet was observed in the
bottom of the centrifuge tube. Most of the iron in these
filtered water samples therefore consists of colloidal
particles of diameter less than 0.45μ ..

f) Colloidal iron model experiment

The iron-organic colloid association was modeled
using a well-characterized colloidal suspension of goethite
(Freundlich and Wosnessensky, 1923) with average particle
dimensions of $0.1 \times 0.01\mu$ (Heller and Peters, 1970). In
a 1:50 dilution with distilled water, the iron in this
suspension will not pass through an 0.45μ filter because
the crystallites clump together to a slight extent. The
use of distilled water filtered through a pre-rinsed
0.05μ filter gives the same result; residual detergents
leaking out of the filter do not stabilize the individual

Table 9. Effect of ultrafiltration and ultracentrifugation
on iron concentration of 0.45µ filtered Mullica River
water.

Treatment	Initial total iron* µmol/l	Final total iron µmol/l	% removed
0.10µ filtration	15.8	4.3	73%
0.05µ filtration	15.8	3.3	79%
30,000g, 2 hr.	12.0	9.2	23%
90,000g, 3 hr.	10.6	2.5	76%

*These experiments were performed on different batches of
 0.45µ filtered river water.

crystallites. A portion of filtered river water was refiltered through a pre-rinsed 0.05μ filter and then mixed with the colloidal suspension in a 33:1 ratio. This mixture was then refiltered through an 0.45μ filter; almost all of the iron remained in the filtrate. The river's dissolved organic matter stabilizes the crystallites and retains iron in solution. When this refiltered mixture was used in seawater mixing experiments as described previously, (with a 45 min. standing time), a salinity dependent precipitation is observed which was similar to that obtained for the naturally-occurring iron (Table 10, Fig. 8). This similarity of behavior supports the hypothesis that river-borne colloidal iron oxide is stabilized by natural organic matter and that this combined iron-organic colloid undergoes a salinity-dependent precipitation in estuaries. The organic stabilization functions by forming an exterior sheath of negatively charged carboxyl groups that form an energy barrier to coagulation (Stumm and Morgan, 1970). In natural systems the colloids are less likely to contain crystalline goethite and are probably amorphous mixtures with domains of hydrated ferric oxide and coprecipitated organic matter (Coey and Readman, 1973).

Conclusions

1) Iron removal has now been observed when river water meets seawater in at least 8 estuaries on 14 occasions.

Table 10. Colloid model mixing experiment.

Salinity ‰	Total iron* μmol/l
0	11.2
2	8.5
5	6.4
9	0.8
14	0.5
18	0.2
28	0.2

0.05μ filtered river water contained 1.4 μmol/liter natural total iron; addition of colloid and filtration through 0.45μ millipore filter raised iron concentration to 11.7 μmol/l.

*measured after filtration through an 0.45μ filter.

Figure 3-8. Colloid model mixing experiment: total
iron vs. salinity in the filtrates.
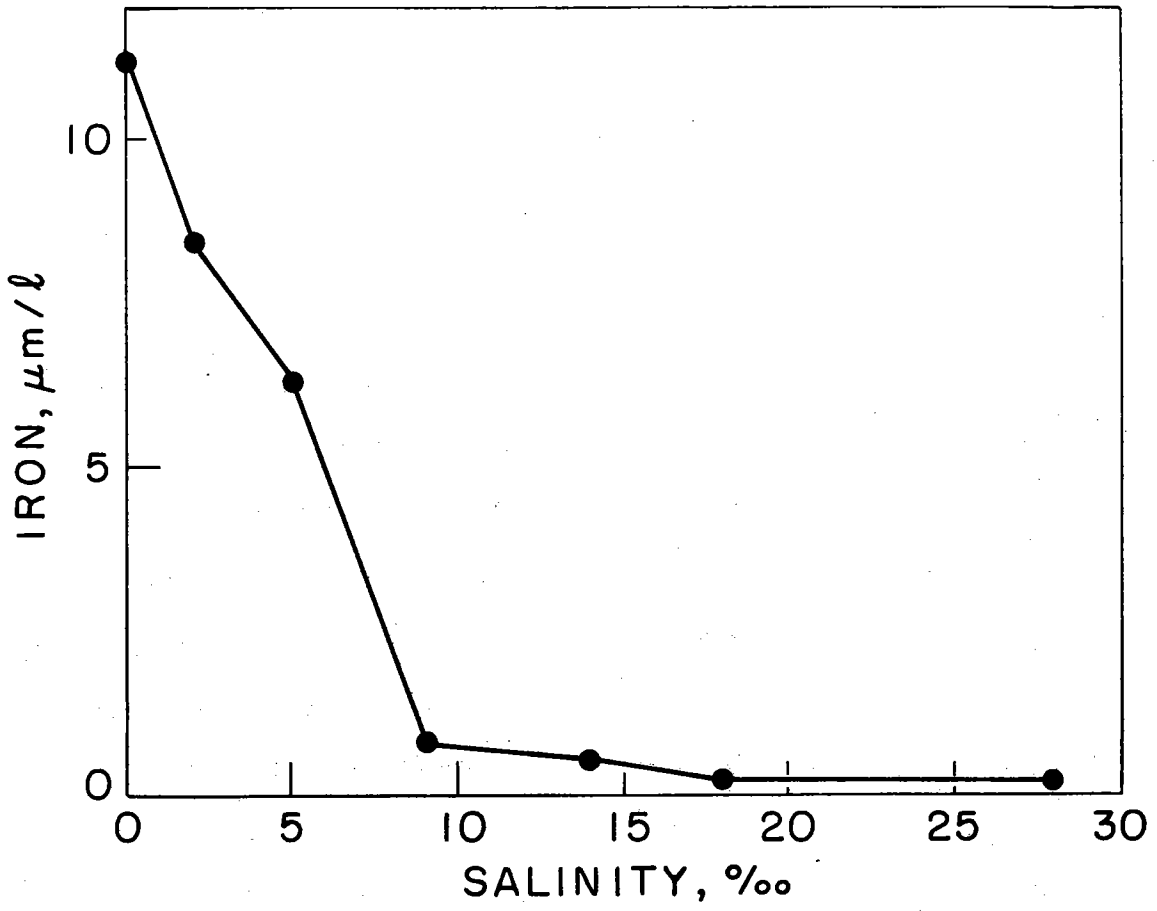
This removal is probably a common phenomenon.

2) In the Mullica river "dissolved" iron consists of mixed iron oxide-organic matter colloids of diameter less than 0.45μ . The dissolved organic matter stabilizes these colloids. When the river water mixes with seawater in the estuary, these negatively charged colloids react rapidly with seawater cations to form a precipitate. The degree of coagulation increases with increasing salinity; further work is required to understand in detail the mechanism of this salinity-dependence.

3) A similar iron precipitation process has been observed in several other estuarine situations and in laboratory experiments. Given the widespread availability of organic matter and iron oxide in most freshwater systems, the same conclusions should apply to these cases.

4) The estuarine precipitation process can be modeled in the laboratory by an organic-stabilized goethite colloid.

5) Mild acidification (pH=2) slowly dissolves the iron oxide; wet chemical analyses may produce low iron analyses if dissolution is not complete. Boiling briefly in the presence of the reducing agent hydroxylamine dissolves the iron oxide and should be employed in analytical procedures for iron (Table 5). Iron released by severe treatment such as autoclaving has been interpreted in the past as "organic" iron. This interpretation is correct to the extent that iron is associated with organic matter; however, the chemical

environment of the iron is more strictly characterizable as
a hydrated ferric oxide phase. Since phosphorus is
probably bound in the colloids as phosphate substituting
for oxygen in the oxide phase (Levesque and Schnitzer,
1967), similar caution should be applied to interpretation
of the difference between total phosphorous and "inorganic
phosphate" (as determined by most analytical procedures for
phosphate which may not completely dissolve the iron colloids)
as "organic phosphorous".

6) The reaction between metal cations and the coagulated
iron-organic colloids may be regarded as a type of organic
complexation. Investigations on the complexing ability of
dissolved organic matter frequently employ metal concen-
trations higher by orders of magnitude than the naturally
occurring levels. At these higher concentration levels the
metal cation may be bound by the organic matter in a
precipitate like those observed in this work rather than as
a soluble complex. Extrapolation of stability behavior
observed in complexing studies at high metal concentrations
to the lower natural levels assuming a _dissolved_ metal-ligand
interaction may lead to erroneous conclusions about the
speciation of the trace metal. Future work in this area
should take care to distinguish between the two effects.

7) As demonstrated here and by Sholkovitz (1976), other
elements - notably, Mn, Al, and P - are bound in the iron-
organic precipitate. These and other species should show a

removal effect in estuaries. This effect may be overwhelmed by a dominance of the soluble form of the element; for example, in the aforementioned ultracentrifugation experiment where 75% of the iron was sedimented, only 6% of the manganese was removed. Some scavenging of soluble constituents by the flocculating colloids may occur but should not be as extensive as expected for freshly-precipitated ferric oxide. The question of the degree to which a constituent is non-conservative in a given estuary must be resolved by field studies and laboratory mixing experiments.

8) In his classic treatise on the chemical composition of freshwater systems, Livingstone (1963) discussed some of the ambiguities involved in iron analysis, but nonetheless went on to compute a world average dissolved iron concentration for rivers of 12μmol/liter. This number has been widely quoted and used in the calculation of the oceanic residence time for iron. The present work and that of Kennedy et al. (1974) make it clear that the iron concentration of a filtered sample depends highly on the pore size of the filter and the degree to which clogging (tab. 5) reduces the effective pore size. The most reproducible iron concentrations would be obtained from the initial filtrate through an unclogged filter of known pore size, but the geochemical significance of even this procedure is not clear, since removal of a large fraction of iron from solution in estuaries rules out the calculation of a meaningful oceanic

residence time based on the primary river input. A large

fraction of the iron in solution is converted from colloids

to larger particles and then is governed by particulate

transport mechanisms. Based on the sampling of estuaries

in this work, the supply of iron to the ocean is reduced

from the primary river concentration to less than 1 μmol per

liter of river water, a number which is an order of magnitude

lower than Livingstone's. The ultimate supply of iron from

the continents may be altered further by other reactions such

as diffusion of iron from the pore waters of shelf sediments.

The above estimate must be understood than as a tentative one.

References

Beck, K.C., J.H. Reuter, and E.M. Perdue (1974), Organic
    and inorganic geochemistry of some coastal plain rivers
    of the southeastern United States, Geochim. Cosmochim. Acta,
    38:341-364.

Bewers, J.M., I.D. Macaulay, and B. Sundby (1974), Trace metals
    in the waters of the Gulf of St. Lawrence, Can. J. Earth
    Sci. 11:939-950.

Boyle, E.A., R. Collier, A.T. Dengler, J.M. Edmond, A.C. Ng,
    and R.F. Stallard, On the geochemical mass balance in
    estuaries, Geochim. Cosmochim. Acta 38:1719-1728.

Carroll, D.(1958), Role of clay minerals in the transportation
    of iron, Geochim. Cosmochim. Acta, 14:1-28.

Coey, J.M.D. and P.W. Readman (1973), Characterisation and
    magnetic properties of natural ferric gel, Earth Plan.
    Sci. Lett. 21: 45-51.

Coonley, L.S. Jr., E.B. Baker, and H.D. Holland (1971) Iron in
    the Mullica River and Great Bay, New Jersey, Chem. Geol.
    7:51-63.

Deb, B.C. (1949), The movement and precipitation of iron oxides
    in podzol soils, J. Soil Sci. 1:112-122.

Eckert, J.M. and Sholkovitz, E.R. (1976) The flocculation of
    iron, aluminum, and humates from river water by electrolytes,
    Geochim. Cosmochim. Acta, in press.

Freundlich, V.H. and S. Wosnessensky (1923); Ueber eisenoxydsole
    die aus eisencarbonyl gewonnen werden, Kolloid Zeitschrift
    33:222-227.

Gjessing, E.T. (1964) Ferrous iron in water, Limnol. Oceanogr. 9:272-274.

Heller, W. and J. Peters (1970), Mechanical and surface coagulation 1: surface coagulation of α-FeOOH sols, J. Col. Interface Sci. 32:592-605.

Hem, J.D. (1960), Complexes of ferrous iron with tannic acid, USGS Water Supply Paper 1459-D.

Irving, H. and R.J.P. Williams (1953), The stability of transition-metal complexes, J. Chem. Soc. 3192-3210.

Jones, B.F., V.C. Kennedy and G.W. Zellweger (1974) Comparison of observed and calculated concentrations of dissolved Al and Fe in stream water, Water Resources Res. 10:791-793.

Kennedy, V.C., G.W. Zellweger, and B.F. Jones (1974), Filter pore-size effects on the analysis of Al, Fe, Mn, and Ti in water, Wat. Resources Res. 10:785-790.

Khan, S.U. (1969) Interaction between the humic acid fraction of soils and certain metallic cations, Soil Sci. Soc. Am. Proc. 33:851-854.

Lamar, W.L. (1968), Evaluation of organic color and iron in natural surface waters, USGS Prof. Paper 600-D, D24-D29.

Levesque, M. and Schnitzer (1967), Organo-metallic interactions in soils: 6. Preparation and properties of fulvic acid-metal phosphates, Soil Sci. 103:183-190.

Lengweiler,V.H., W. Buser, and W. Feitknecht (1961), Die ermittlung der löslichkeit von eisen (III) - hydroxiden mit ^{59}Fe II. Der zustand kleinsten mengen eisen (III) hydroxid in wässeriger lösung, Helv. Chim. Acta 44:805-811.

Lewin, J. and C. Chen (1973), Changes in the concentration of soluble and particulate iron in seawater enclosed in containers, Limnol. Oceanogr. 18:590-596.

Livingstone, D.A. (1963), Chemical composition of rivers and lakes, USGS Professional Paper 440-G.

Martin, D.F., M.T. Doig, and R.H. Pierce, Jr. (1971), Distribution of naturally occurring chelators (humic acids) and selected trace metals in some west coast Florida streams, 1968-1969, University of South Florida Professional Papers Series #12.

McMahon, J.W. (1967), The influence of light and acid on the measurement of ferrous iron in lake water, Limnol. Oceanogr. 12:437-442.

Perhac, R.M. (1972), Distribution of Cd, Co, Cu, Fe, Mn, Ni, Pb, and Zn in dissolved and particulate solids from two streams in Tennessee, J. Hydrol. 15:177-186.

Phillips, C.S.G. and R.J.P. Williams (1966), Inorganic Chemistry, vol. II, pp. 80-82.

Rainwater, F.H. and L.L. Thatcher (1960), Methods for collection and analysis of water samples: U.S. Geol. Survey, Paper 1454.

Rashid, M.A. (1971) Role of humic acids of marine origin and their different molecular weight fractions in complexing di- and tri-valent metals, Soil Sci. 111:298-306.

Schnitzer, M. and W.A. Delong (1955), Investigations on the mobilization and transport of iron on forested soils. II. The nature of the reaction of leaf extracts and leachates with iron, Soil. Sci. Soc. Am. Proc. 19:363-368.

Schnitzer, M. and S.I.M. Skinner (1963a), Organo-metallic interactions in soils: 1. Reactions between a number of metal ions and the organic matter of a podzol B_n horizon, Soil Sci. 96:86-93.

_____(1963b), Organo-metallic interactions in soils 2. Reactions between different forms of iron and aluminum and the organic matter of a podzol B_n horizon, Soil Sci. 96:181-186.

_____(1965), Organo-metallic interactions in soils: 4. Carboxyl and hydroxyl groups on organic matter and metal retention, Soil Sci. 99:278-284.

Segar, D.A. and A.Y. Cantillo (1975), Direct determination of trace metals in seawater by flameless atomic absorption spectrophotometry, in Analytical Methods in Oceanography (ed. Gibb), Advances in Chemistry Series 147, American Chemical Society, pp. 56-81.

Shapiro, J. (1958), Yellow acid-cation complexes in lake water, Science 127:702-704.

Shapiro, J. (1966), On the measurement of ferrous iron in natural waters, Limnol. Oceanogr. 11:293-298.

Shapiro, J. (1964) Effect of yellow organic acids on iron and other metals in water, Am. Wtr. Wrks. Assoc. Journal 55:1062-1082.

Sholkovitz, E.R. (1976), Flocculation of dissolved organic and inorganic matter during the mixing of river water and seawater, Geochim. Cosmochim. Acta, in press.

Stookey, L.L. (1970) Ferrozine: a new spectrophotometric reagent for iron, Anal. Chem. 42:779-781.

Strachov, N.M. (1948), Distribution of iron in lake sediments

   and the factors of its control, Akad. Nauk SSSR, Ser.

   Geol. Izv. no. 4, pp. 3-50.

Stumm, W. and J.J. Morgan (1970), Aquatic Chemistry, Wiley-Interscienc

   pp. 282-294, pp. 492-493, and p. 500.

Theis, T.L. and P.C. Singer (1974), Complexation of iron (II) by

   organic matter and its effect on iron (II) oxygenation,

   Env. Sci. Tech. 8:569-573.

Windom, H.L., K.C. Beck, and R. Smith (1971) Transport of trace

   elements to the Atlantic Ocean by three southeastern rivers,

   Southeast. Geol., pp. 1109-1181.

***------
Omitted Reference

Ong, H.L. and R.E. Bisque (1968) , Coagulation of Humic
   colloids by metal ions, Soil Sci. 106: 220-224.

Chapter 4

The Marine Geochemistry of Cadmium

The marine geochemistry of trace consituents like cadmium is geochemically interesting because of the marked vertical and geographical gradients observed for species of short oceanic residence times. Secondarily, an understanding of the cadmium cycle is necessary because of the potentially detrimental effects associated with cadmium pollution (1).

Previous efforts to elucidate the behavior of cadmium in the ocean have produced no systematic correlations with other oceanographic properties (2), probably because of problems with analysis and contamination during sampling. Recent advances in technique have led to progress in our understanding of other trace metals (3,4,5) and a re-examination of the distribution of cadmium is now appropriate. This note describes the distribution of cadmium in the ocean based on three detailed vertical profiles from the Pacific Ocean.

Station locations were chosen to cover a broad range of oceanographic conditions, from the Antarctic circumpolar current (Stn 293) to the temperate mid-Pacific (Stn 226) and the North Pacific upwelling region in the Bering Sea (Stn 219) (Table 1). The samples were taken using rosette-mounted 30 1 PVC Niskin bottles with epoxy coated internal springs and stored in acid-leached polyethylene containers following acidification to pH=2. The handling of containers and samples is described in detail elsewhere (4). Cadmium was preconcentrated from

100g samples by cobalt pyrrolidine dithiocarbamate coprecipitation (6) and analyzed by heated graphite atomizer atomic absorption spectrometry (7). The estimated precision and accuracy of the analysis is $\pm$ 0.1 nanomole/kg. The cadmium data together with relevant hydrographic information is listed in table 1.

Depth profiles of cadmium are shown in figure 1 along with profiles of the nutrients phosphate and silicate. It is readily apparent that cadmium is depleted in the surface ocean relative to the deeper waters. Such a distribution is indicative of involvement in the biogeochemical cycle of surface uptake by organisms and regeneration from sinking biological debris deeper in the ocean. The total range of variation in concentration is at least a factor of ten, from 0.1 $\pm$ 0.1 to 1.1 $\pm$ 0.1 nmol/kg.

The cadmium profiles resemble those of phosphate more than silicate: the concentrations increase rapidly with depth to a maximum at about 1 km and then decrease slightly below this. The covariance with phosphate is consistent between all stations (figure 2) and suggests that cadmium, like phosphate and nitrate, is regenerated in a shallow cycle rather than deeper in the ocean as is silicate.

The results are compatible with some recent cadmium data. Bender and Gagner (5) report numbers for the surface (0.05 nm/kg) and deep (0.30 nm/kg) Sargasso Sea; Knauer

Table 1   Hydrographic data from 3 Pacific Geosecs Stations.

Station 219   10/8/73   177° 17.5' W   53° 6.6' N

DEPTH meters	POTENTIAL TEMPERATURE °C	SALINITY ‰	SILICATE µmol/kg	PHOSPHATE µmol/kg	CADMIUM nmol/kg
5	7.107	33.069	32.2	1.60	0.61
160	3.533	33.524	74.2	2.42	0.96
349	3.548	33.886	100.8	2.89	1.13
460	3.417	34.027	113.7	2.97	0.96
599	3.294	34.159	128.0	3.03	1.14
642	3.226	34.177	131.0	2.89	1.04
792	3.047	34.266	141.9	2.89	1.05
943	2.834	34.337	150.9	3.04	1.16
1189	2.531	34.413	163.3	2.95	1.09
1440	2.249	34.480	176.5	3.05	1.05
1677	1.983	34.536	190.1	3.01	1.15
1988	1.741	34.585	202.7	2.98	1.04
2287	1.594	34.613	209.5	2.91	1.08
2583	1.482	34.635	214.6	2.89	1.08
3480	1.310	34.665	226.9	2.80	1.03
3711	1.281	34.669	221.7	2.74	0.99

Table 1, (cont'd)

DEPTH meters	POTENTIAL TEMPERATURE °C	SALINITY ‰	SILICATE μ mol/kg	PHOSPHATE μ mol/kg	CADMIUM nmol/kg
Station 226	11/9/73	170° 36.5' E, 30°34.0' N.			
8	24.73	35.055	3.3	0.02	0.12
36	24.75	35.053	2.7	0.01	0.09
82	23.58	35.005	3.2	0.02	0.20
207	15.19	34.627	7.2	0.49	0.13
382	12.01	34.396	16.0	0.89	0.27
456	10.33	34.277	23.8	1.15	0.20
555	7.92	34.103	38.5	1.61	0.36
591	7.28	34.066	45.6	1.76	0.54
687	5.62	34.031	68.5	2.29	0.89
982	3.62	34.265	121.6	2.97	0.89
1126	3.20	34.371	135.3	3.02	1.08,1.06
1274	2.85	34.440	145.0	3.03	0.96,0.89
1421	2.53	34.488	153.7	3.00	0.92
1712	2.06	34.560	165.1	2.89	0.88
2442	1.48	34.639	163.5	2.67	0.61
3005	1.28	34.663	154.7	2.58	0.61
3785	1.141	34.679	149.7	2.47	0.65
4175	1.095	34.685	147.9	2.43	0.78
4361	1.075	34.684	145.7	2.43	0.81
4779	1.03	34.689	139.9	2.36	0.60
5446	0.971	34.695	136.2	2.33	0.78

Table 1 (cont'd)

Station 293   3/1/74   178° 5.0' W,   52°40.0' S

DEPTH meters	POTENTIAL TEMPERATURE °C	SALINITY ‰	SILICATE μ.mol/kg	PHOSPHATE μ mol/kg	CADMIUM nmol/kg
3	11.328	34.419	2.7	0.72	0.13
216	7.65	34.419	5.2	1.28	0.31, 0.38
458	6.46	34.342	6.6	1.40	0.20
685	5.27	34.268	17.6	1.76	0.46
961	4.07	34.312	30.8	2.00	0.71, 0.73
1143	3.30	34.347	44.8	2.13	0.98
1290	2.83	34.395	53.8	2.24	0.91
1587	2.45	34.525	68.9	2.28	0.83
1733	2.37	34.577	73.4	2.27	0.87
2029	2.19	34.659	80.3	2.19	0.78
2326	2.018	34.708	83.7	2.10	1.07, 1.12, 1.29
2621	1.78	34.732	88.5	2.06	0.96
2771	1.65	34.763	91.9	2.06	0.61
3065	1.422	34.735	98.3	2.08	0.66
3509	1.05	34.723	108.7	2.10	0.77
4019	0.77	34.711	116.6	2.13	0.80
4474	0.586	34.705	120.5	2.15	0.82
4926	0.48	34.700	124.5	2.16	0.98, 1.26
5271	0.446	34.699	125.3	2.17	0.92

Figure 4-1. Cadmium, phosphate, and silicate
profiles for three stations in
the Pacific Ocean.

o   : silicate

●   : phosphate

STN 219
CADMIUM, nmol/kg

STN 226
CADMIUM, nmol/kg

STN 293
CADMIUM, nmol/kg

SILICATE, μmol/kg

SILICATE μmol/kg

SILICATE, μmol/kg

PHOSPHATE, μmol/kg
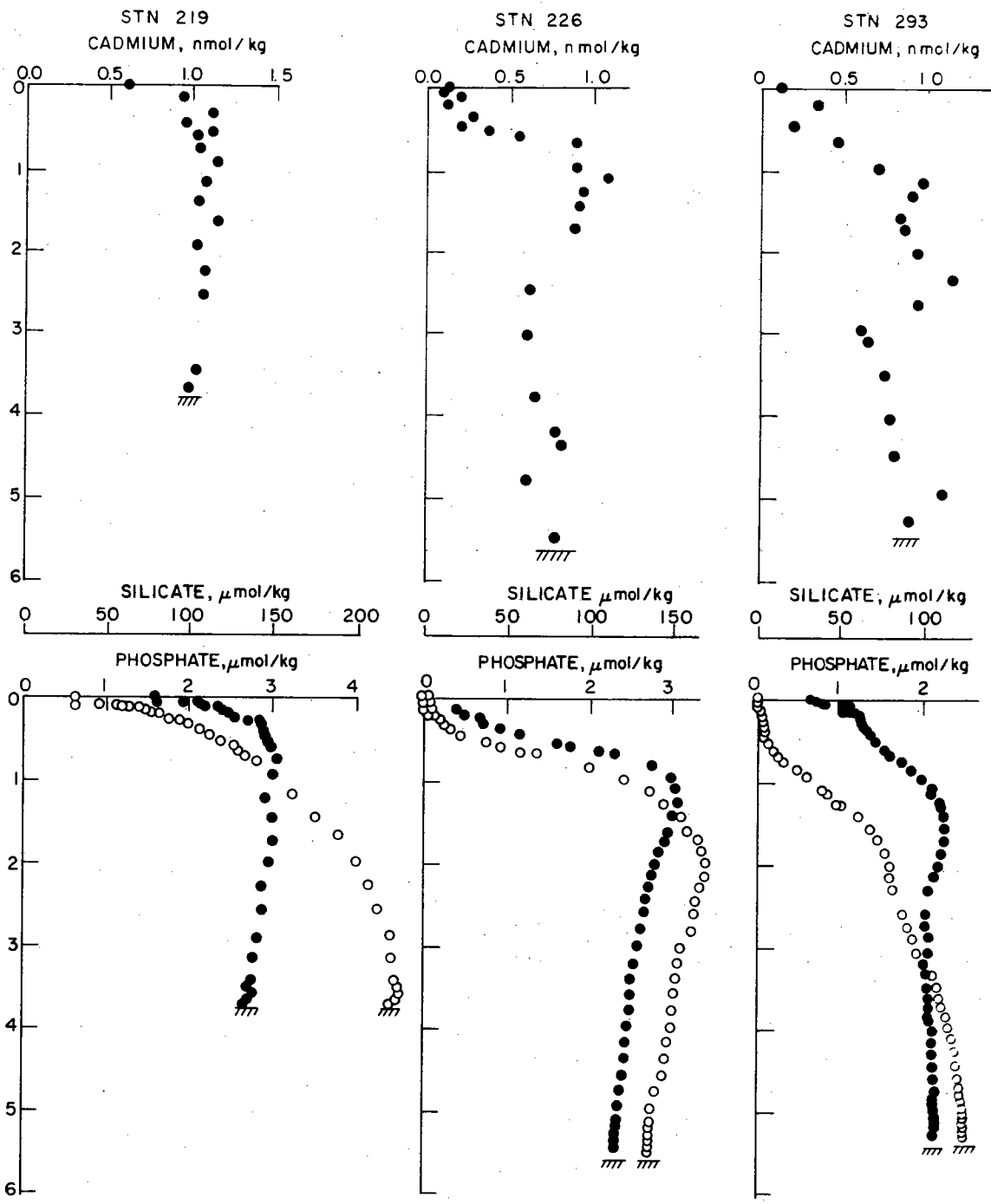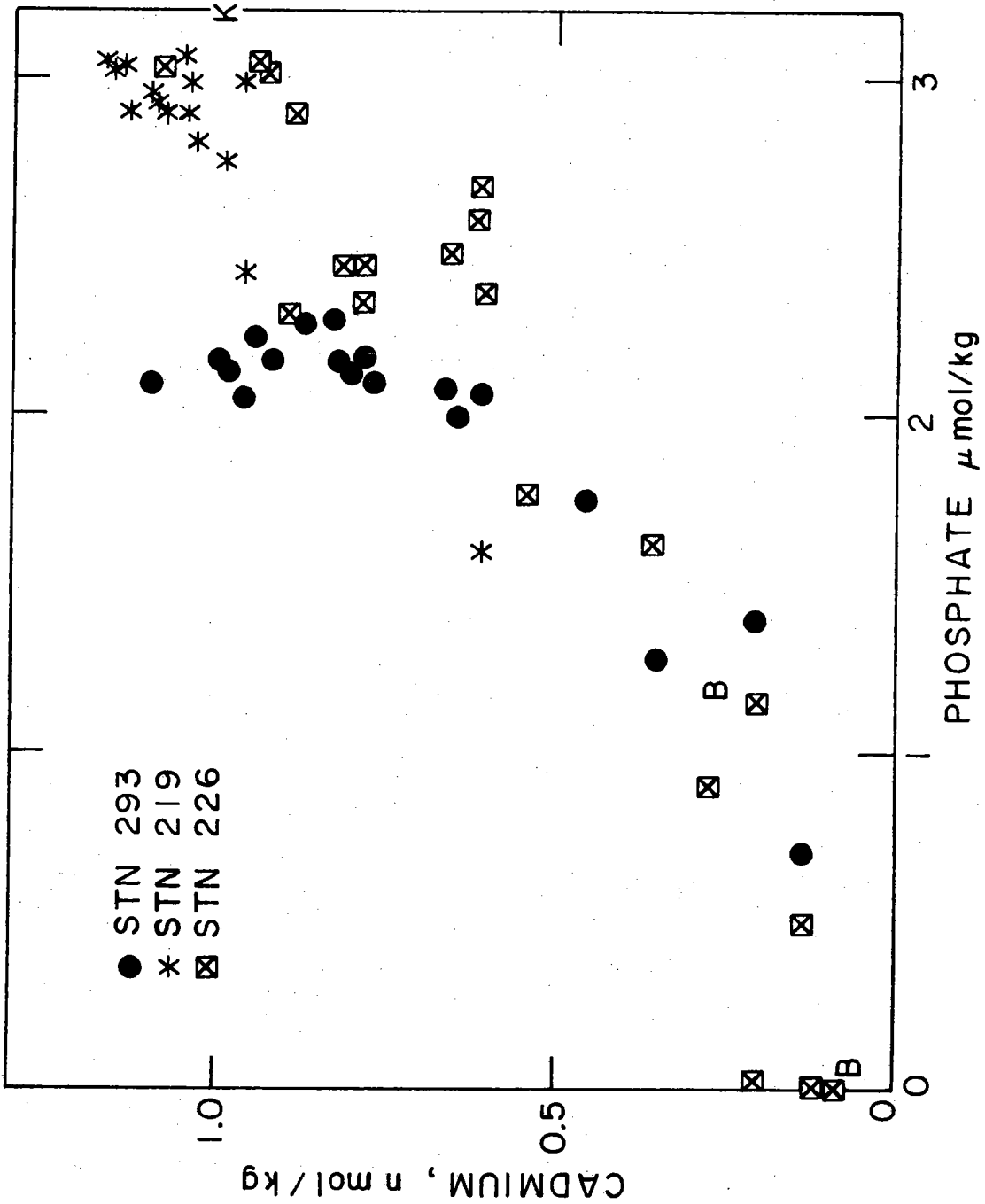
PHOSPHATE, μmol/kg

PHOSPHATE, μmol/kg

Figure 4-2. Cadmium vs. phosphate for three Pacific
profiles and three data points from the
literature.   B and K represent cadmium
data from references 5 and 8, respectively.

and Martin (8) give one number at 1000 m depth near
Hawaii (1 nm/kg) and report surface concentrations below
their detection limit (0.2 nmol/kg). Estimates of the
phosphate concentrations at these locations were made
using data from nearby GEOSECS stations. These numbers
are plotted in figure 2. The agreement is excellent.
The cadmium-phosphate correlation observed in these
stations probably holds throughout the world ocean.

A detailed comparison of the chemical composition
of plankton with the hydrographic correlation of cadmium
and phosphate is not possible because there are few
analyses including both elements. Goldberg et. al. (9)
report analyses of _Sargassum_ and planktonic animals
with Cd:P molar ratios of 4×10^{-4} and 6.5×10^{-4} respectively.
These values are close to the water column ratio (3.5×10^{-4}).
Martin and Broenkow (11) observed cadmium enrichments of
a factor of 3 in plankton from the Baja California upwelling
region relative to organisms in the open Pacific. Cadmium,
like phosphate, is enriched in the surface waters of
upwelling regions (e.g. Stn 219). The phosphate content
of the Baja California waters is about a factor of 3 higher
than further away from the coast (12), and a similar
enrichment should apply to the cadmium concentration in
these waters. It is evident th the cadmium content of
plankton depends on the concentration in the water in which
the organisms grow. A mechanistic interpretation of the
cadmium-phosphate correlation requires information on the

site of incorporation of cadmium in organisms and sinking biogenic debris. Similar depth profiles would result if cadmium were contained in either the soft tissues of organisms or in rapidly-dissolving hard parts such as celestite ($SrSO_4$) (10). Future work on the chemical composition of marine plankton should attempt to isolate the location of the various elements in the organisms.

Lastly, it should be noted that there is no evidence in these data for cadmium pollution in the open ocean. Indeed, the efficient scavenging of this metal by organisms will rapidly remove pollutant cadmium from the mixed layer so that it should not present a serious environmental problem for oceanic organisms away from localized sources of cadmium.

References

(1) McCaull, J. (1971) , Building a shorter life,
Environment 13(7) : 2-16.

(2) Brewer, P.G. (1975) , Minor elements in Seawater, in:
Chemical Oceanography, second edition, J.P. Riley and G.
Skirrow, eds., Vol. 1, Ch. 7, p. 415.

(3) Boyle, E.A. and J.M. Edmond (1974), Copper in
surface waters south of New Zealand, Nature 253:107-109.

(4) Sclater, F., E. Boyle, and J.M. Edmond (1976),
On the marine geochemistry of nickel, Earth Plan.
Sci. Lttrs, in press.

(5) Bender, M.L. and C.L. Gagner (1976), Dissolved
copper, nickel and cadmium in the Sargasso Sea,
J. Mar. Res., in press.

(6) Boyle, E.A. and J.M. Edmond (1975, Determination of
Trace Metals in aqueous solution by APDC chelate-
co-precipitation, in: Analytical Methods in Oceanography
ACS Advances in Chemistry Series #147, pp. 44-55.

(7) Chapter 2, this thesis.

(8) Knauer, G.A. and J.H. Martin (1973), Seasonal
variations of cadmium, copper, manganese, lead, and
zinc in water and phytoplankton in Monterey Bay
California, Limnol. Oceanogr. 18:597-604.

(9) Goldberg, E.D., W. S. Broecker, M.G. Gross, and
K.K. Turekian, Marine Chemistry, in: Radioactivity
in the Marine Environment, National Academy of Sciences,
1971, p. 144.

(10) Brass, G.W. and K.K. Turekian (1974), Strontium
distribution in GEOSECS oceanic profiles, Earth Plan.
Sci. Lett. 23: 141-148

(11) Martin, J.M. and W.W. Broenkow (1975), Cadmium in
plankton: elevated concentrations off Baja California,
Science 190:884-885.

(12) Dugdale, R.C. and M.L. Healy (1971), University
of Washington, Department of Oceanography Technical
Report #250; F.R. Richards, 1970, University of Washington
Technical Report #249.

Chapter 5

The Marine Geochemistry of Copper and Nickel

Introduction

Elements which are involved strongly in the cycle
of surface uptake by organisms and deep regeneration from
sinking biological debris show marked vertical and
horizontal variations throughout the ocean. The concentration
levels are controlled by a dynamic balance between the
rates of continental supply, biological uptake, recycling,
and ocean circulation (1). For this reason the distributions
of these elements are sensitive to variations in the global
environment. An understanding of the mechanisms controlling
their present distributions will have an important bearing
on the interpretation of their sedimentary records and hence
in the construction of paleo-oceanographic models.

Classically there were only a handful of elements with
known variable distributions independent of total salt:
$C, O_2, N, P,$ and Si. The last decade has seen the introduction
of a number of stable and radioactive species to the list
of oceanographic variables (2,3). None of these were
transition elements, however. Yet these latter display
a remarkable diversity of properties and can serve as
indicators of redox processes (Cr, Mn, Fe), provide
information on the mode of formation of manganese nodules
(Mn,Fe,Cu,Ni,Co), and exert an influence on the growth
of organisms (all of the first-row transition elements
with the possible exception of Sc, Ti, and Ni). The reason

for the paucity of information is not lack of effort
but rather the severe problems with sample collection
and analysis that result from the extremely low concentration
levels encountered. Advances in analytical techniques and
improvements in sampling methods have led recently to the
first valid information on the distribution of a few
transition metals (3,4,5,6).

In order to help bridge this gap in the geochemical
cycle, copper and nickel measurements have been made for
three detailed vertical profiles from the north and south
Pacific Ocean. The nickel data complements recent work
(4) while the copper measurements constitute the first
extensive suite of data on the distribution of this
element. Additionally, an estimate for the continental
supply rate has been derived by measurements of copper
and nickel in the Amazon estuary.

Methods

Samples profiles were collected in rosette mounted
30 liter PVC Niskin bottles with epoxy-coated internal
springs. The samples were originally collected for barium
analysis as part of the GEOSECS program (4).

The Amazon estuary samples were collected during a
cruise of the R/V CHAIN in June, 1974; the ship cruise
track is published elsewhere (7). Most of the samples
were collected by vacuum-pumping through polyethylene
tubing from a towed "fish", streamed off the side of the

ship using a boom, into acid-leached polyethylene bags.
A few samples were obtained from wire-mounted 30 liter
Niskin bottles with teflon-coated internal springs. The
nickel data from the Niskin samplers were consistently
higher than the "fish" samples and were excluded.
Samples were acidified to pH 2 shortly after collection
by addition of redistilled 6N hydrochloric acid. The
copper and nickel analyses reported here are only for
unfiltered samples. Water for barium analyses was taken
from "bucket" samples collected while steaming, and a
few were taken from Niskin bottles. Samples were filtered
through acid-leached glass fiber filters, a procedure which
introduces negligible contamination for this element.

Copper and nickel determinations were made on 100 ml
samples by graphite atomizer flameless atomic absorption
spectrometry (8) after preconcentration by cobalt pyrrolidine
dithiocarbamate chelate coprecipitation (9). The estimated
analytical precisions of the analyses are Cu, $\pm$ 0.2
nanomole/kg , and Ni, $\pm$ 0.3 nm/kg. For the higher copper
concentrations encountered in the Amazon estuary the
estimated precision for copper is $\pm$5%. The accuracy of
the analyses is estimated to be comparable to the precision.

Barium analyses were made by isotope-dilution mass
spectrometry (10). The precisi . and accuracy is better
than $\pm$1% (11).

Salinity determinations on the estuarine samples were
made with a refractometer (estimated precision $\pm$ 0.2‰)

Station locations and hydrography

The general water-column distributions of chemical
properties are strongly influenced by the physical processes
of advection and mixing. It is thus necessary to understand
something of the hydrographic conditions to interpret chemical
profile data. The nutrients phosphate and silicate in
particular serve well as tracers of the effect of physical
processes on chemical distributions.

Station 293 is located south of New Zealand just north
of the Antarctic circumpolar front. The surface silicate
concentration is low (1.8 μm/kg) and increases regularly
through the intermediate and deep water masses into the
Antarctic bottom water; phosphate values are moderately
high (0.69 μm/kg) at the surface, and increase with depth
to a maximum at 1500 m (figure 1). The bottom water at
this station is representative of the source waters for
the northward-flowing deep western boundary current and,
modified by subsequent mixing with shallow waters, of the
deep water of the entire Pacific.

Station 345 is located south of San Diego approximately
400 km west of the tip of Baja California. Surface nutrient
levels are moderately low (Si=5.2,P=0.25,NO_3 < 0.1). The
characteristics of the deeper waters are dominated by the
sluggish circulation of the northeast Pacific. The silicate
concentration increases to a broad deep maximum (3.2 km)
and decreases very slightly to the bottom due to renewal

of the bottom water by remnants of the bottom boundary current flowing through the Line Island-Hawaii Gap. The distribution of phosphate is distinct from that of silicate as it increases rapidly to a sharp maximum at 900 meters. Below 1 km the potential temperature-salinity relation is linear.

Station 219, in the Bering Sea, has the highest observed silicate levels in the ocean (228 um/kg) at 3600 m. The deep water flows into the basin from around the Aleutian Arc near the Kamchatka Peninsula. The silicate decrease in the bottom 100 m is evidence for active near-bottom water renewal. A linear potential temperature - salinity relation obtains below 1400 m. Surface nutrient levels are high in this upwelling region (Si=32, P=1.6).

Validity of the data

A-priori arguments on the extent of precautions in sampling and analysis are not in themselves sufficient to establish the validity of trace metal data. The primary criterion is oceanographic consistency. In practice this means that detailed profiles must show smooth variations that are consistent with the hydrography and show sensible geographic variations. Erratic "spikes" are an indication of bad data.

On this basis the profiles from stations 219 and 293 can be judged reliable; they both show regular variations with the deviations from smooth curves comparable to the estimated analytical precision (figure 1). For station 345, however, 3 copper data points and 4 of those for

nickel (out of a total of 18) are "erratics" (table 1).
The problem was traced to dirty bottle caps. If the
erratics are discarded, distributions consistent with
those observed at other stations are obtained. Nonetheless,
in view of the problems encountered at this station, the
discussion is based on the other stations. The deep
water copper data from station 345 is used, however,
because the station is ideally located for advection-
diffusion modeling.

The distribution of nickel

Based on data from four profiles from the Atlantic
and Pacific Sclater, Boyle, and Edmond (4) have established
the general distribution of nickel in the ocean. The
concentrations vary in a fashion similar to the nutrients,
being depleted in the surface relative to the deep waters.
The form of the profiles is not exactly the same as that
observed for either phosphate or silicate, however, and
was shown as being best described by a dual covariance
with the two nutrients:

$$Ni = 3.3 + (1.1 \times 10^{-3})P + (3.3 \times 10^{-5})Si$$

This result can be interpreted as due to regeneration in
both a shallow cycle (like P) and a deep cycle (like Si).
This correlation is not mechanistic and does not imply any
chemical assocation of Ni with P or Si.

The data presented here (figure 1) are generally
consistent with the above conclusions, but certain differences
are notable. At the Antarctic station 293, the Ni(P, Si)

Table 1   Hydrographic data from 3 Pacific Geosecs Stations

Station 219   10/8/73   177° 17.5' W, 53° 6.6' N   Depth 3734 m

DEPTH Meters	POTENTIAL TEMPERATURE °C	SALINITY ‰	SILICATE µm/kg	PHOSPHATE µm/kg	NICKEL nm/kg	COPPER nm/kg	BARIUM nm/kg
5	7.107	33.069	32.2	1.60	6.1	2.61	57.1
160	3.533	33.524	74.2	2.42	6.5	3.12	67.8
349	3.548	33.886	100.8	2.89	7.4	3.07	75.3
460	3.417	34.027	113.7	2.97	8.1	2.76	---
599	3.294	34.159	128.0	3.03	7.2	3.02	84.6
642	3.226	34.177	131.0	2.89	8.4	2.53	---
792	3.047	34.266	141.9	2.89	7.6	2.57	96.0
943	2.834	34.337	150.9	3.04	8.5	2.76	103.6
1189	2.531	34.413	163.3	2.95	10.0	3.92	112.4
1440	2.249	34.480	176.5	3.05	9.6	3.30	122.0
1667	1.983	34.536	190.1	3.01	10.6	3.77	130.8
1988	1.741	34.585	202.7	2.98	8.6	3.54	144.6
2287	1.594	34.613	209.5	2.91	11.3	4.09	148.6
2583	1.482	34.635	214.6	2.89	11.2	4.31	154.2
3480	1.310	34.665	226.9	2.80	10.4	5.59	162.2
3711	1.281	34.669	221.7	2.74	10.8	6.03	160.8

Table 1 (cont'd)

Station 293   3/1/74   175° 5.0' W, 52° 46.0' S   Depth 5454 m

DEPTH Meters	POTENTIAL TEMPERATURE °C	SALINITY ‰	SILICATE µm/kg	PHOSPHATE µm/kg	NICKEL nm/kg	COPPER nm/kg	BARIUM nm/kg
3	11.328	34.419	2.7	0.72	4.1	1.59	45.8
216	7.65	34.419	5.2	1.28	4.5,4.7	1.28,1.14	47.9
458	6.46	34.342	6.6	1.40	5.0	1.22	54.5
685	5.27	34.268	13.1	1.63	5.9	1.87	58.7
961	4.07	34.312	38.0	2.00	5.8,6.2	2.48,2.17	67.0
1143	3.30	34.347	44.8	2.13	7.0	1.99	75.4
1290	2.83	34.395	53.8	2.24	7.4	1.82	-71.0
1587	2.45	34.525	68.9	2.28	8.0	2.28	81.4
1733	2.37	34.577	73.4	2.27	7.2,7.1	2.25,2.19	82.5
2029	2.19	34.659	80.3	2.19	6.9	2.45	85.5
2326	2.018	34.708	83.7	2.10	7.8	2.85	85.2
					7.0	2.63	
					7.1	2.74	
2621	1.78	34.732	88.5	2.06	6.9	2.55	88.7
2916	1.52	34.736	95.8	2.08	6.3	2.44	90.8
3065	1.422	34.735	98.3	2.08	7.8	3.14	94.0
3509	1.05	34.723	108.7	2.10	7.3	3.26	98.0
4019	0.77	34.711	116.6	2.13	7.9	3.96	99.5
4474	0.586	34.705	120.5	2.15	7.4	3.93	99.6
4926	0.48	34.700	124.5	2.16	8.2,7.8	4.55,4.08	101.5
5271	0.446	34.699	125.3	2.17	7.2	4.36	103.6

Table 1 (cont'd)

Station 345   6/6/74   122° 12.8' W, 22° 31.5' N   Depth 4221 m

| DEPTH Meters	POTENTIAL TEMPERATURE °C	SALINITY ‰	SILICATE µm/kg	PHOSPHATE µm/kg	NICKEL nm/kg	COPPER nm/kg
11	18.418	34.157	5.2	0.25	4.1	1.40
67	16.910	33.958	5.8	0.26	8.4*	1.12
136	12.511	33.775	10.4	0.68	3.7	1.87
186	10.702	33.885	23.4	1.57	6.2	2.77
274	9.590	34.296	38.8	2.32	11.2*	2.49
343	8.275	34.286	50.8	2.51	6.0	2.58
424	7.424	34.364	62.8	2.82	7.4	3.60
505	6.364	34.328	75.4	2.92	10.7*	5.08*
584	6.102	34.417	81.3	3.02	8.0	2.37
786	4.997	34.469	100.3	3.14	11.4*	7.00*
995	4.114	34.511	117.8	3.16	9.3	2.80
1291	3.251	34.561	135.2	3.08	10.5	2.84
1590	2.638	34.596	146.0	2.99	11.5	3.27
1887	2.140	34.622	156.1	2.82	10.4	3.26
2183	1.787	34.646	161.4	2.78	10.9	7.69*
2581	1.536	34.661	164.9	2.69	12.7	4.80
3775	1.205	34.681	165.6	2.54	10.2	5.69
4203	1.193	34.681	164.7	2.53	9.3	5.52

* Contamination suspected

Figure 5-1. Profiles of copper, nickel, phosphate,

and silicate for two GEOSECS stations

in the Pacific Ocean
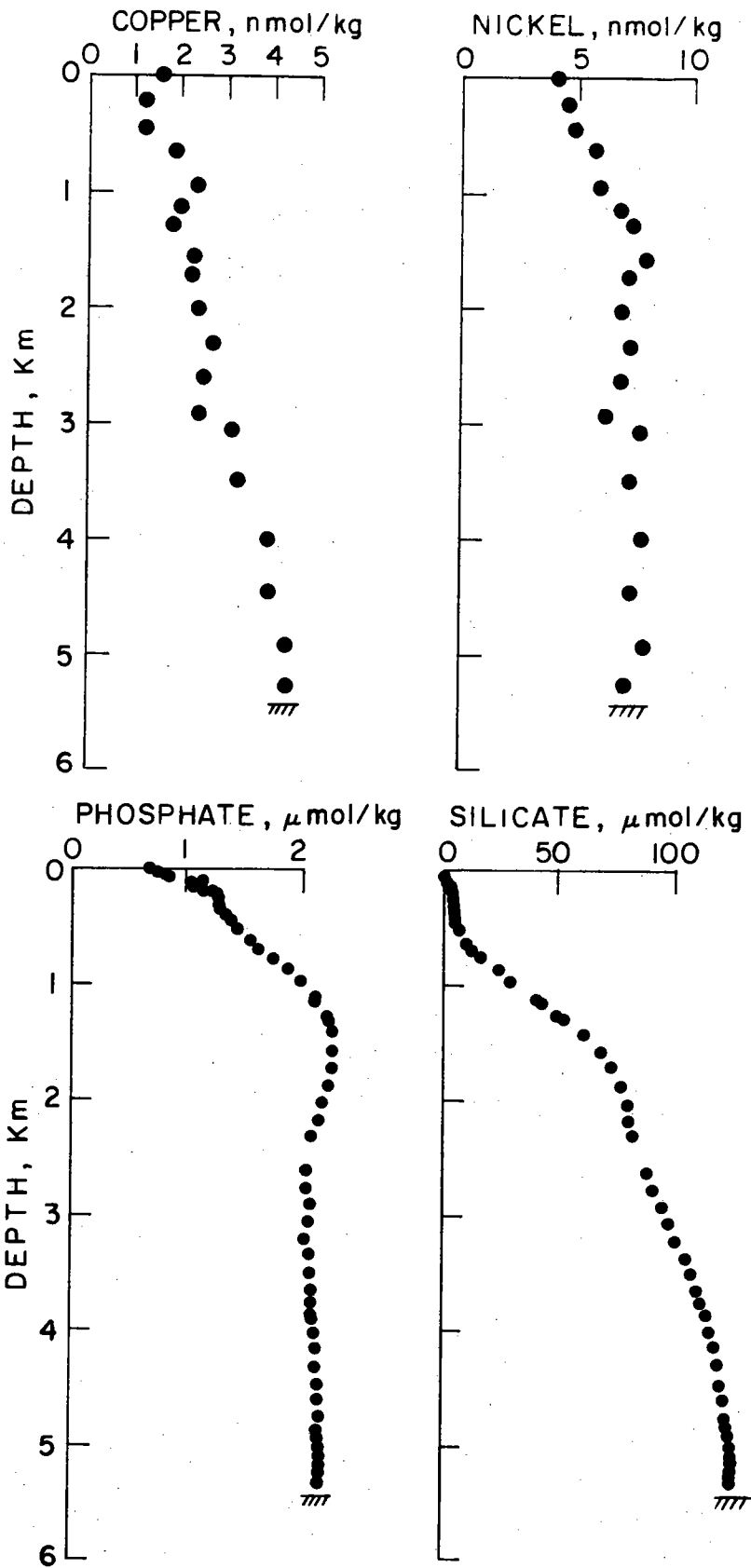
A) Station 219, Bering Sea

B) Station 293, South of New Zealand

A
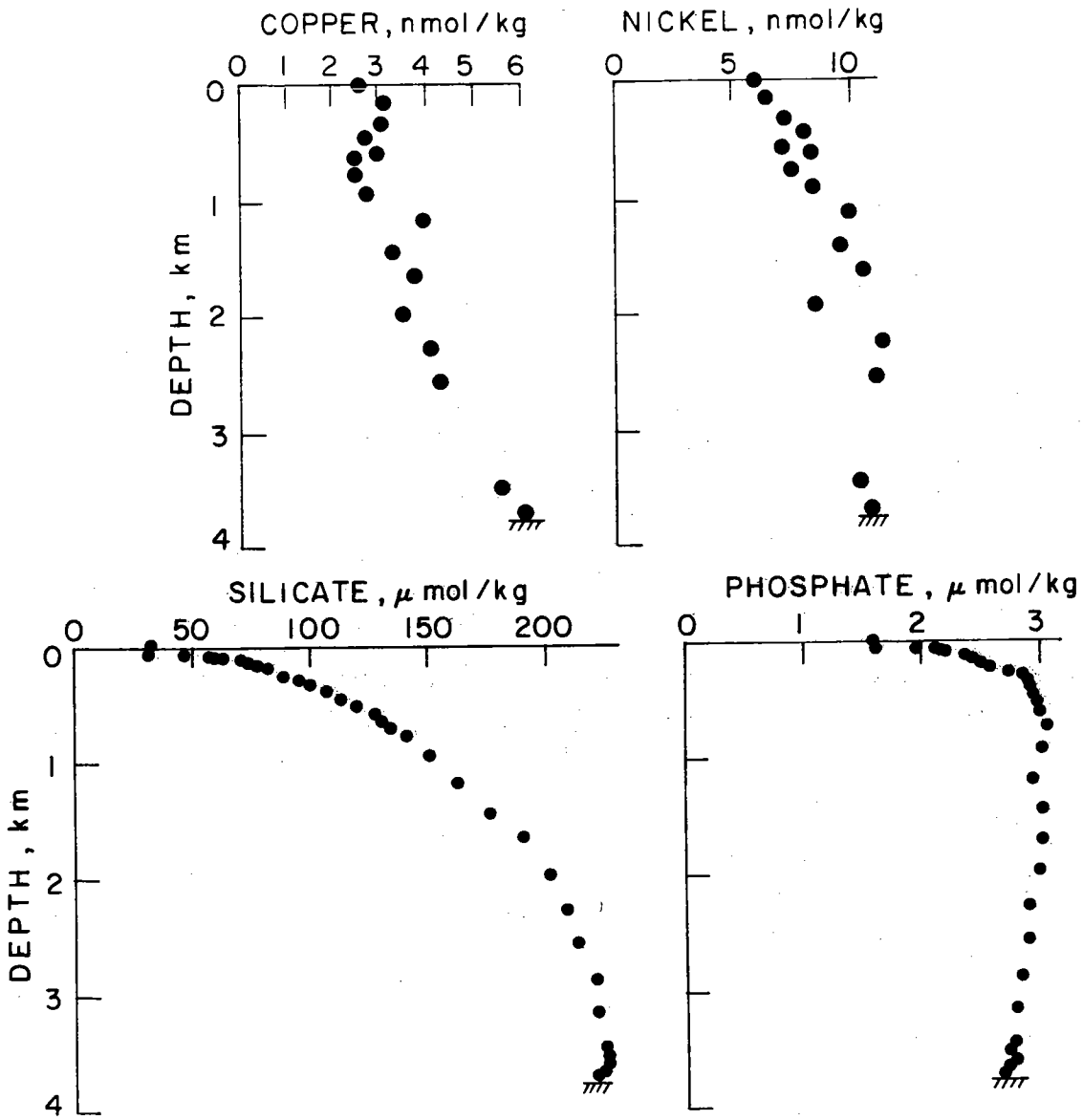
GEOSECS STN 219

GEOSECS STN 293

relationship of Sclater et. al. (4) is consistent with observations in the upper water column but predicts levels higher than observed, by 2 nm/kg, in the deep water. The form of the profile at this station is better fit by a linear combination of silicate and phosphate covariance than either nutrient separately, but the apparent silicate cofactor is lower than observed for the north Pacific stations of Sclater et. al.

Alkalinity and Barium also show linear relationships with silicate in mid-ocean regions that differ from the relation for the Antarctic. In both cases the difference is such that compared to the mid-Pacific the antarctic surface waters have more barium (or alkalinity) at a given silicate concentration, whereas in the deep water the reverse is observed. The effect of this relationship is to diminish the slope of the barium or alkalinity vs. silicate line in the Antarctic. The primary cause of the Antarctic relationship is an excess of silicate uptake (relative to barium or alkalinity) near the surface due to increased diatom productivity accompanied by an excess flux of silicate into the bottom water. A similar effect is observed for the barium-silicate relationship in the deep water of the Bering Sea (Stn 219).

The deviation of the Antarctic and Bering Sea stations from the northeast Pacific Ni(P,Si) relationship is due to this effect. Alkalinity or barium should display a more consistent correlation with nickel than does silicate.

Since barium is measured with greater precision
'relative to the observed a range of variability), nickel
data from GEOSECS stations 343, 204, 293, and 219 have
been fit to a linear combination of phosphate and barium:

$$Ni = 1.3 + (1.3 \times 10^{-3})P + (4.1 \times 10^{-2})Ba.$$

As observed by Sclater et. al. (4), the additional variance
explained by the addition of the phosphate covariance is
statistically significant (F=34; critical F at $P_{.001} = 12$).
A few contaminated samples near the phosphate maxima could
also produce this relationship, but the likelihood is small
that this would happen both in these stations and those of
Sclater et. al. Hence the conclusion that nickel is
regenerated in both a shallow cycle (like P) and a deep
cycle (like Ba) is substantiated by the data from these
stations. Of the total range of variability (3 to 12 nm/kg)
approximately one-third is related to shallow regeneration
and the rest to deep regeneration. It should be emphasized
that the relationships between nickel and the other elements
indicate only that the _rates_ of surface removal and subsequent
regeneration are similar, and that no mechanistic association
is necessary.

The distribution of copper

Previous information of the distribution of copper is
limited to 10 surface samples from the Pacific Antarctic
upwelling region (3) and surface and "deep" samples from
the Sargasso Sea (5). In the antarctic surface data copper

is linearly correlated with phosphate, nitrate, and alkalinity but not with silicate. The nutrient covariance demonstrates that copper is removed from the surface ocean by organisms and released at depth. If the correlation with nitrate is in fact valid, copper should occur at very low levels (less than 0.1 nm/kg) in surface waters of the central gyres (3). But Bender and Gagner (5) showed that Sargasso Sea surface water contains 1.5 nmCu/kg. The profile data from the stations reported here (figure 1) are also inconsistent with a general correlation with nitrate: copper maxima are not observed at the nitrate maxima and the copper concentrations always increase with increasing depth. Copper must be regenerated very deep in the water column or from the bottom. Such a consistent increase to the bottom is not found for other species known to be regenerated in a deep cycle: these all show deep maxima induced by the circulation of younger bottom water with lower concentration levels than the older deep water.

The copper behavior in the deep water column can be represented by a simple physical model. Stations 219 and 345 have linear potential temperature-salinity relationships in the deep water with an exponential depth variation for both properties. Such relationships can be explained consistently (though not uniquely) by a steady-state vertical advection-diffusion model with constant coefficients (13,14,15). The general equation describing this model is

$$1) \quad \frac{\partial c}{\partial t} = -w \frac{\partial c}{\partial z} + K \frac{\partial^2 c}{\partial z^2} + J = 0$$

where z and w are positive downwards and J is a zero-order
in situ consumption or production rate. A zero order
dependence was chosen because the data is not sufficiently
detailed or precise to justify more complicated expressions.
The general solutions of this equation for potential
temperature (θ) and the concentration of the chemical species
of interest are

2) $\theta = a + be^{+(w/k)z}$

3) $C = m + \frac{J}{w} z + ne^{+(w/k)z}$

where a,b,m, and n are integration constants. Rearranging
eq'n (1), substituting into eq'n (2), and combining integration
constants gives

4) $C = \alpha + \frac{J}{w} z + \beta\theta$

where α and β are the combined integration constants. Using
this formulation J/w can be determined simply by a multiple
linear regression of the concentration data vs. θ and z.
This procedure has the advantage of simplicity of calculation
and requires no assumptions about end-member concentrations.

Plots of copper vs. potential temperature for these
two stations are shown in figure 2. If the chemical reaction
term J is zero, the Cu-θ relationship should be linear. Instead,
the Cu-θ plot shows a negative curvature indicative of in-situ
copper consumption. The data from these stations were fit
to equation (4) to derive estimates for J/w. The curve fits
are plotted in the figure as well as fits for J/w = $\pm50\%$ of the
best fit. An estimate for the value of J for station 345
can be made by using the value of w determined for a nearby

Figure 5-2. Copper vs. potential temperature for
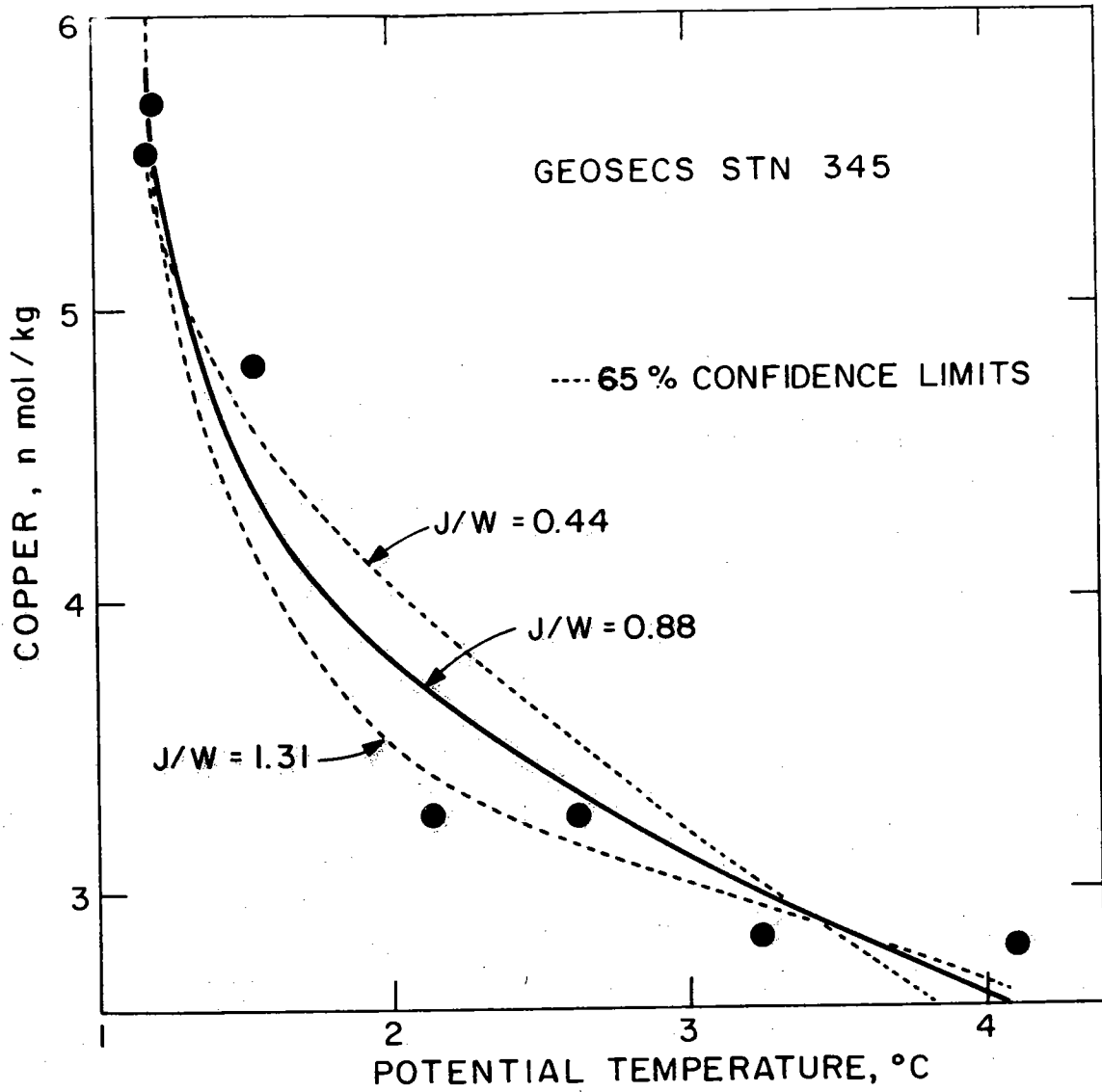two GEOSECS stations in the Pacific
Ocean.

A) Station 219, Bering Sea

B) Station 343, Eastern Pacific near
Baja California.

A

GEOSECS STN 219

----- 95 % CONFIDENCE LIMITS

J/W = 0.82

J/W = 1.64

J/W = 2.43

POTENTIAL TEMPERATURE, °C
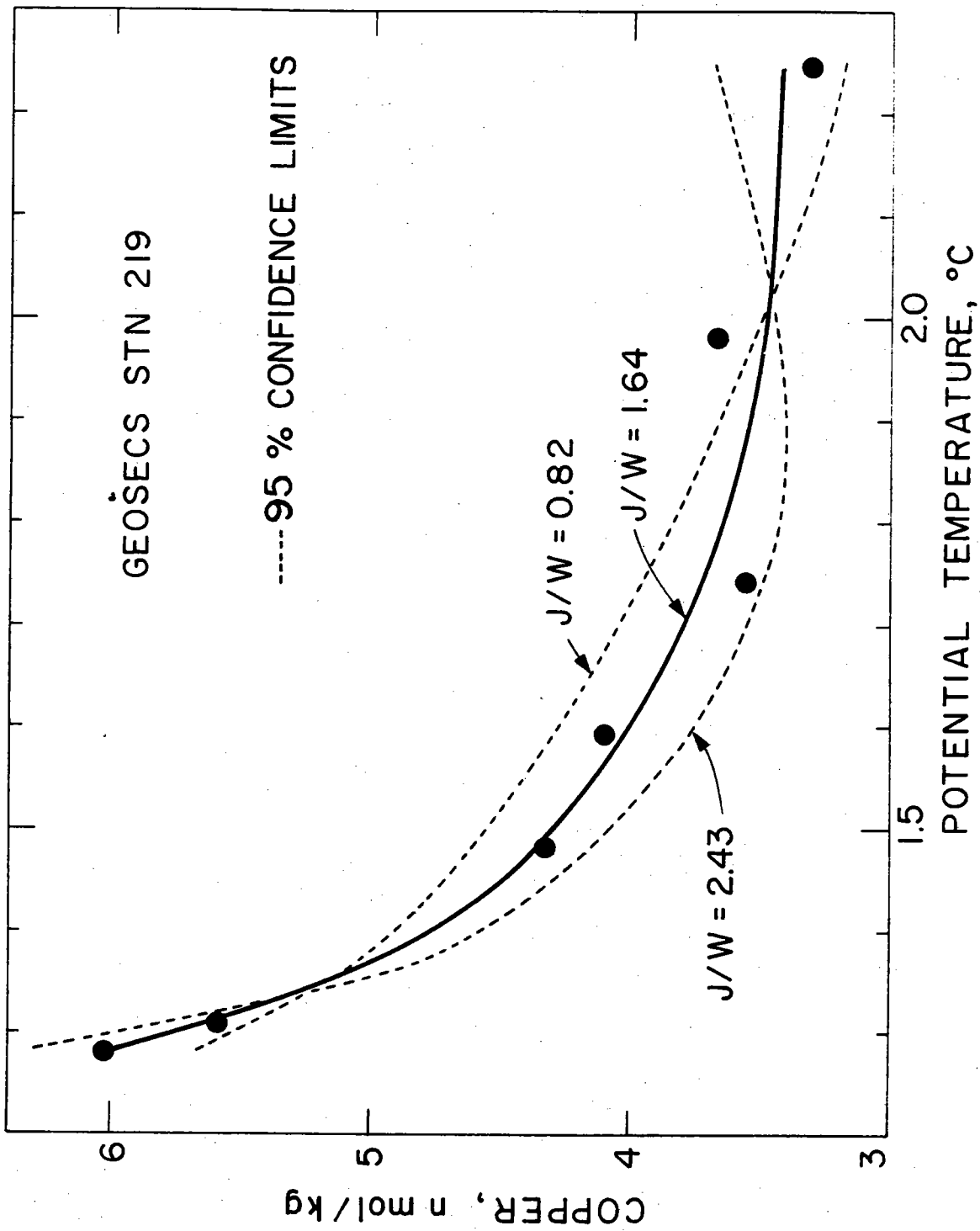
COPPER, n mol/kg

station -3.7 m/yr.,(16) The apparent in-situ scavenging

rate is 3.2×10^{-3} nmol/kg /yr. The scavenging residence

time for copper in the deep water is then about (4.5 nm/kg

/ J) ≃ 1400 years.

There are several possible effects which could invalidate

the results of a simple one-dimensional model (14, 16).

The most serious problem is circulation where strong horizontal

gradients exist. The station coverage is not sufficient at

present to rule out this possibility. The similarity at two

widely separated stations as well as the absence of such a

distribution for any other property argues against such an

effect. Another model problem is the possibility of the

diffusion of a localized effect into the water column which

produces an apparent in-situ scavenging rate related to distance

from the sink. This anomaly is a less serious problem as it

is still consistent with scavenging of copper from the deep

ocean.

Additional evidence for the scavenging effect is provided

by the comparison of copper with barium (figure 3). At station

219 the copper-barium relationship is linear up to a certain

barium concentration beyond which the copper concentration

increases abruptly while barium increases only slightly. A

similar relationship with barium has been observed for radium

in the northeast Pacific (17). In the case of radium the

curvature at high barium values is explained by diffusion of

primary radium out of the bottom and subsequent radioactive

decay in the water column (18). For copper a similar

relationship is generated by in-situ scavenging rather than

Figure 5-3. Copper vs. Barium for two stations in the

Pacific Ocean.
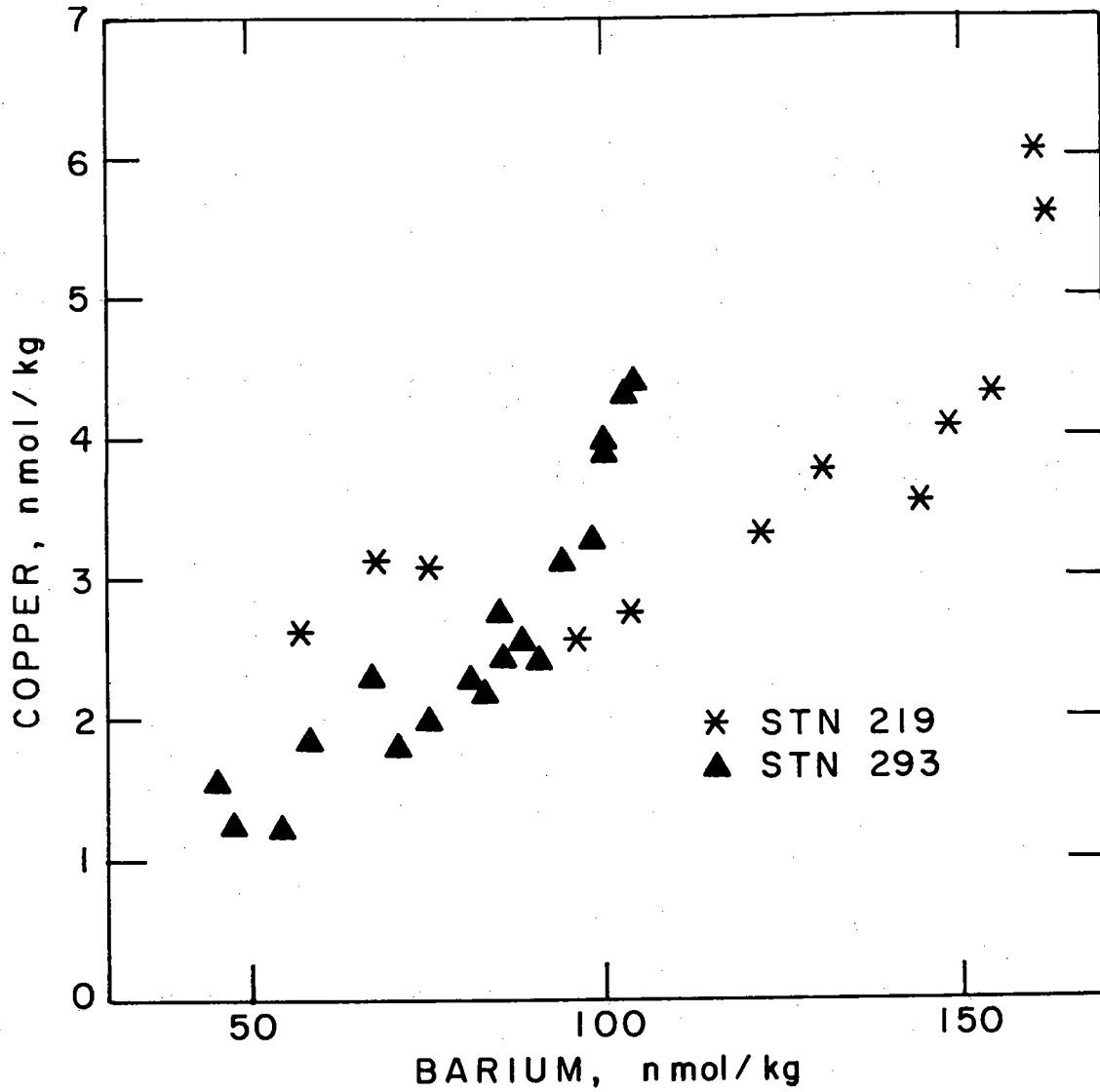
radioactive decay. But the mean scavenging time for copper (1400 years) is considerably shorter than the mean life of radium with respect to radioactive decay. (2341 yrs.) For this reason the copper vs.barium plot shows upward curvature in the deep water in the Antarctic at Stn 293 (fig. 1) while radium does not (18): the higher rate of circulation there compared to the northeast Pacific obsures the radium decay anomaly.

The flux from the bottom required to balance the in-situ deep water scavenging and the surface uptake by organisms at station 345 is estimated by the method of Munk (14) as

$$F_B = WC_B + K\frac{\partial c}{\partial z} = 6 \ nm/cm^2/yr$$

assuming $K=1 \ cm^2/sec$ and $w= -3.7 \ m/yr$. With an effective sediment diffusion coefficient of $10^{-6} \ cm^2/sec$ this flux requires a pore-water gradient near the sediment surface of 200 nm/kg/cm ! Such high gradients cannot extend very deep into the sediment as the solubility product of CuO (tenorite) would be reached within a few centimeters (19). The profile data thus requires a very strong source of copper near the sediment surface.

The dualistic behavior of copper with mid-depth scavenging and a flux from the bottom sediment poses mechanistic problems. Evidently particles take up copper while falling yet release copper after reaching the bottom. This behavior is contrary to that of the radioactive isotope ^{210}Pb which is also scavenged from the water column. Bacon (20) demonstrated that the distribution of this radioisotope,

which is generated by in-situ decay of ^{226}Ra, can be
modeled consistently by scavenging at the bottom followed
by horizontal diffusion of the scavenging anomaly. One
possible solution to the copper dilemna is that different
types of particles are responsbile for the two processes,
For example, biogenic debris may carry copper to the
bottom and release it into solution while another type of
particle, perhaps Fe-Mn oxides from hydrothermal vents at
mid-ocean ridge crests, scavenge copper. The possibility
that the copper scavenging effect is due to coprecipitation
in hydrothermal iron-manganese sediments deserves serious
consideration.

If the apparent in-situ scavenging rate is taken as
the average for the entire eastern Pacific ocean below 1 km
(volume ~ 2 x 10^8 km^3) and is considered to be due to
deposition of copper along the East Pacific Rise (length ~
6 x 10^3 km) with a width of deposition of Fe-Mn sediments
of about 1000 km (25) then the average copper accumulation
rate in the region of the ridge crest would be 1 x 10^{-8}
moles/cm^2/yr. This estimate, probably reliable to no more
than an order of magnitude is a factor of ten higher than
observed rates on the East Pacific Rise (25). The estimate
would tend to be high because the station is much closer to
the ridge crest than the average for the Eastern Pacific.
If ridge-crest scavenging of copper is important, systematic
copper depletions decreasing with increasing distance from
the ridge should be observed, as for the input anomaly of

^{3}He (22).

Copper and Nickel in the Amazon Estuary

The continental input of copper and nickel was estimated
by measurements in an estuarine region because reactions in
this zone can alter significantly the net flux of dissolved
material. Removal of iron from solution has been observed
in a number of estuaries (23) and desorption of barium has
been reported for the Mississippi estuary (24). Barium is
also desorbed in the Amazon estuary (tab. 2, fig. 4). This desorptioi
process doubles the net flux of dissolved barium into the
ocean and illustrates the importance of estuarine reactions
for the budgets of trace constituents. Since filtered samples
were shown to be contaminated for copper and nickel, a similar
desorption process could not be verified for these metals.
However, because river-borne particulate material is rapidly
sedimented from the Amazon estuary (7), the net input of
dissolved material can be obtained from unfiltered samples
in the outer,high salinity reaches of the mixing zone.

Nickel shows a linear relationship with salinity that
extrapolates to a net input (25) of 6.7 nm/kg of river water.

The copper flux decreases through the mixing zone. At
salinities <20‰ the net input is 24.5 nm/kg of river water.
At higher salinities the input i 17.8 nm/kg. The decrease
with increasing salinity may be due either to a particulate
copper decrease as the total particulate concentration
decreases or to biological consumption of copper in the

Table 2   Data from the Amazon Estuary, June 1974

DATE,TIME (local)	DEPTH m	SALINITY ‰	COPPER nm/kg	NICKEL nm/kg
16-0905	0	5.6	19.1	6.9
16-0835	0	8.6	20.9,17.4,19.0	5.2,5.9,5.4
16-2230	4	10.6	15.6	
12-1500	0	12.5	14.5,17.1	4.7,4.5
16-0310	0	16.3	11.6	4.4
12-0830	0	18.7	8.4,11.0	3.6,3.7
17-0330	5	19.3	18.7	
17-1750	0	22.0	7.2,7.6	4.2,4.3
18-0810	0	28.8	5.6	2.9
19-0930	0	30.5	4.8	2.7
19-1330	0	32.5	2.7	2.8
12-1930	10	29.8	4.1	
12-1930	20	34.2	2.0	
12-1930	30	35.0	2.2	
12-2100	50	36.2	1.2	

Table 2 (cont'd)

DATE, TIME (local)	DEPTH m	SALINITY ‰	BARIUM nm/kg
Macapa, 5/26/74			
16-2150	0	0.0	129.3
16-1805	0	0.2	189.2
16-1635	0	0.5	149.3
16-1415	0	1.0	149.0,148.7
16-1415	0	1.3	208.5,204.3
16-1550	0	1.6	148.6
16-1205	0	2.4	221.3
16-1130	0	3.2	222.0
16-1000	0	4.6	229.7
16-0900	0	4.8	231.1
16-2230	2	5.6	242.6,236.8
16-0805	0	9.2	181.2
17-1200	0	12.5	178.8
17-1310	0	15.2	180.1
17-1400	0	16.6	144.7
17-1440	0	18.5	139.0
17-1740	0	22.0	105.6
18-0725	0	26.1	91.0
18-0845	0	29.9	73.9
19-1330	0	32.7	63.6
17-1300	58	37.0	41.8

Figure 5-4.   Amazon Estuary Data

        A) Barium vs. Salinity.

        B) Nickel vs. Salinity.

        C) Copper vs. Salinity.
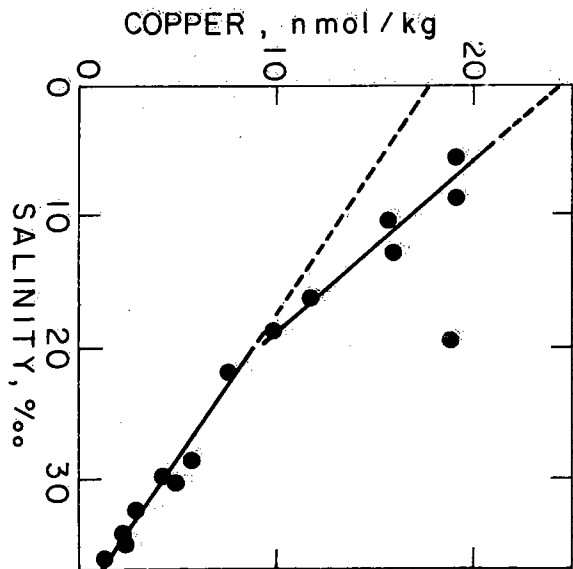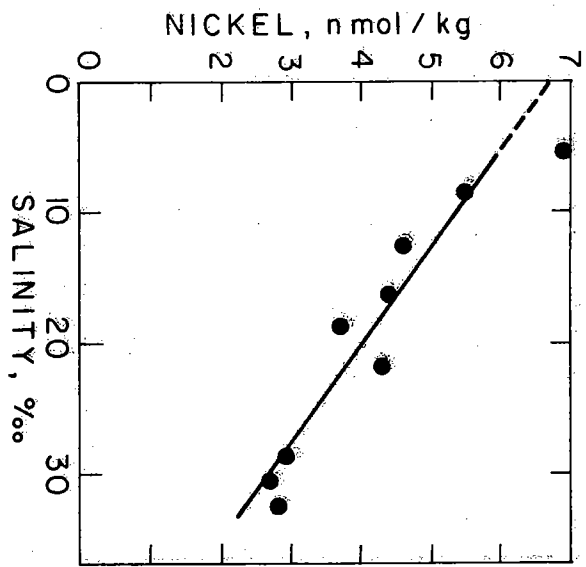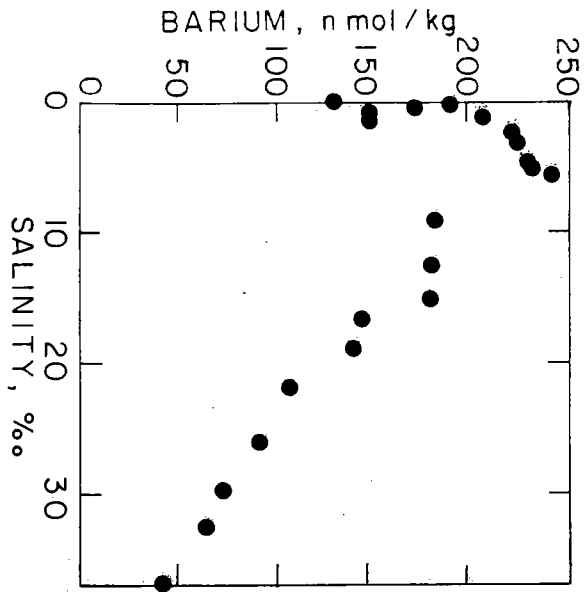
region of high diatom productivity where silica removal is

'served (7).

The oceanic residence time of copper and nickel

Sclater et. al. (4) discussed the oceanic residence
time for nickel and estimated a value of 10,000 years;
the data presented here does not alter their conclusions
in any significant way.

Similar calculations have been made for copper and
are presented in table 3 . The estimates of input and
output differ considerably and indicate that either the
copper concentration of the Amazon is too low to be
representative of world rivers or Pacific pelagic sediments
contain more copper than average oceanic sediments. The
apparent in-situ scavenging residence time is also much shorter
than the river residence time, although this inequality could
be due to spatial variability in the scavenging rate. The
residence time for copper is approximately 10,000 years, a
time comparable to other reactive components: alkalinity
(10^4 yr.), silica (2×10^4 yr) and barium (10^4 yr) (17).

Table 3

Calculation of the Oceanic residence time of copper

	Assumed Avg. Conc.	Total Cu moles	Flux moles/yr	Residence Time yrs.
Ocean	4 nm/kg	5.6×10^{12}		
River Input*	18 nm/kg	--	5.7×10^{8}	1×10^{4}
Sediment Output**	740 ppm	--	6.3×10^{9}	9×10^{2}

* Assumes the Amazon input as representative of world rivers. Turekian (26) compiled a range of freshwater values of 14-190 nm/kg.

** Average pacific pelagic sediment (carbonate-free) (27) multiplied by an assumed avg. sedimentation rate of 0.15 $gm/cm^2/10^3$ yrs multiplied by the area of the ocean.

Conclusions

The marine geochemical cycle of nickel is controlled
by surface uptake by organisms and regeneration in both
shallow (like P) and deep (like Ba) cycles. The rate of
removal from the surface and input into the deeper water
are proportional to a linear combination of the corresponding
rates for phosphate and barium. The mechanism producing
this relationship has yet to be resolved, but must be
determined by the sites into which organisms incorporate nickel.

The ocean chemistry of copper is more complex than
that observed for other species. The dominant processes
controlling its distribution are:

    (1) uptake of copper from the surface by organisms,

    (2) regeneration from biological debris on the bottom,

    (3) mid- and deep-ocean scavenging by an unknown mechanism,

    (4) physical circulation processes.

The net effect is to produce a water-column distribution for
copper that is similar to radium, for which radioactive decay
substitutes for scavenging. The effective mean life for
copper (~1400 yrs) is shorter than that of radium (2341 yrs)
and this difference is reflected in the profile data. The
scavenging mechanism is not known, but may possibly involve
coprecipitation in hydrothermal metal-rich ridge crest
sediments.

The conclusions presented here are based on the net variations throughout the water column. It is possible that the observed net changes are a resultant of simultaneous addition and removal processes. There is no direct evidence for such opposing processes in these data; however, their possible occurrence should be kept in mind.

References

(1) Broecker, W.S., A kinetic model for the chemical composition of seawater, Quaternary Res. $\underline{1}$(1971) 188-207

(2) Broecker, W.S., Chemical Oceanography Harcourt, Brace, Jovanovich, Inc., New York, (1974), 214 p.

(3) Boyle, E.A. and J.M. Edmond, Copper in surface waters south of New Zealand, Nature 253(1975) 107-109.

(4) Sclater, F.R., E. A. Boyle and J.M. Edmond, On the marine geochemistry of nickel, Earth Plan. Sci. Letters, in press (1976)

(5) Bender, M.L. and C.L. Gagner, Dissolved copper, nickel, and cadmium in the Sargasso Sea, J. Mar. Res., in press (1976).

(6) Chapter 4, this thesis

(7) Milliman, J. and E. Boyle, Biological uptake of dissolved silica in the Amazon River estuary, Science 189(1975) 995-997.

(8) Chapter 2, this thesis.

(9) Boyle, E.A. and J.M. Edmond, Determination of trace metals in aqueous solution by APDC chelate coprecipitation, in: Analytical Methods on Oceanography, Advances in Chemistry Series #147, American Chemical Society (1975).

(10) Bacon, M.P. and J.M. Edmond, Barium at Geosecs III in the southwest Pacific, Earth Plan. Sci. Letters $\underline{16}$ (1972) 66-74.

(11) Chan, L.H., D. Drummond, J.M. Edmond, and B. Grant, On the barium data from the Atlantic GEOSECS expedition, submitted to Deep Sea Research (1976).

(12) Edmond, J.M., On the dissolution of carbonate and silicate in the deep ocean, Deep Sea Res. $\underline{21}$(1974) 455-480.

(13) Wyrtki, K., The oxygen minima in relation to ocean circulation, Deep Sea Res. $\underline{9}$(1962)11-28

(14) Munk, W., Abyssal recipes, Deep Sea Res. $\underline{13}$(1966) 707-730.

(15) Craig H., Abyssal carbon and radiocarbon in the Pacific, J. Geophys. Res. 74(1969) 5491-5506.

(16) Craig, H., A scavenging model for trace elements in the deep sea, Earth Plan, Sci. Letters $\underline{23}$ (1974)149-159.

(17) Chan, L.H., J.M. Edmond, R.F. Stallard, W.S. Broecker, Y. Chung, and T.L. Ku, Radium and Barium at GEOSECS stations in the Atlantic and Pacific, submitted to Earth Plan. Sci. Latters (1976)

(18) Li, Y.-H., T.-L. Ku, G.G. Mathieu, and K. Wolgemuth, Barium in the Antarctic Ocean and Implications regarding the marine geochemistry of Ba and ^{226}Ra, Earth Plan, Sci. Letters 19(1973) 352-358.

(19) Murray, J. and P.G. Brewer (1976), The mechanisms of removal of iron, manganese and other trace metals from seawater, in: "Marine Manganese Deposits"(ed. Glassby),Elsevier,in press.

(20) Bacon, M.P., Applications of Pb-210/Ra-226 and Po-210/ Pb-210 disequilibria in the study of marine geochemical processes, Ph.D. Thesis, Joint Program, Woods Hole Oceanographic Institution and Massachusetts Institute of Technology,(1975)

(21) Bostrom, K., T. Kraemer, and S. Gartner, Provenance and accumulation rates of opaline silica, Al, Ti, Fe, Mn, Cu, Ni, and Co in Pacific pelagic sediments, Chem. Geol. 11(1973)123-148.

(22) Craig, H., W.B. Clarke, and M.A. Beg, Excess He-3 in deep water on the East Pacific Rise, Earth Plan. Sci. Letters 26(1975) 125.

(23) Chapter 3, this thesis.

(24) Hanor, J. and L.H. Chan, Behavior of barium during mixing of Mississippi river and Gulf of Mexico water, Geol. Soc. Am. abstracts 7(1975) 1098-1099.

(25) Boyle,E.A., R. Collier, A.T. Dengler, J.M. Edmond, A.C. Ng, and R.F. Stallard, On the chemical mass balance in estuaries, Geochim. Cosmochim. Acta 38 (1974) 1719-1728.

(26) Turekian, K.K., Rivers, tributaries, and streams, in: Impingement of Man on the Oceans (ed. Hood), Wiley, p.9-73, 1971.

(27) Goldberg, E.D. and G. Arrhenius, Chemistry of Pacific Pelagic Sedments, Geochim. Cosmochim. Acta 13(1958)153-212.

Chapter 6

Conclusions:

Comments on the Factors Controlling Trace

Metal Distributions

Previous chapters have been concerned with the
distributions of copper, nickel, and cadmium in the ocean.
This chapter will attempt a brief synthesis of the information
on factors controlling the distributions of trace metals in
general. Presently there is information on the oceanic
variations of four trace metals: Ba, Cu, Ni, and Cd. There
are similarities in the variations of these elements. They
all are involved in biological cycling and show lower
concentrations in the surface relative to the deep ocean.
Yet in detail the distribution of each trace met·l is
different from the others. The best illustration of this
statement is seen in the profiles at GEOSECS Stn 219 (figure 1).
These differences can serve as clues to the mechanisms
operating to produce the observed variations.

The zero-order interpretation of the trace-metal distributions
is that some are regenerated in a shallow cycle, like
phosphorus or nitrate (e.g. Cd) and others are regenerated
in a deep cycle, like silicate or alkalinity (e.g. Cu, Ba).
Nickel is an intermediate case showing variability related
to both shallow and deep regeneration. Mechanistically
this observation requires that metals are bound in distinct
sites in the falling biogenic d·'ris and that these sites
have different recycling rates. The actual sites are not
yet determined. Rapid recycling could be expected for soft

Figure 6-1. Profiles of copper, nickel, cadmium, and

barium from GEOSECS station 219 in the

Bering Sea

GEOSECS STN 219
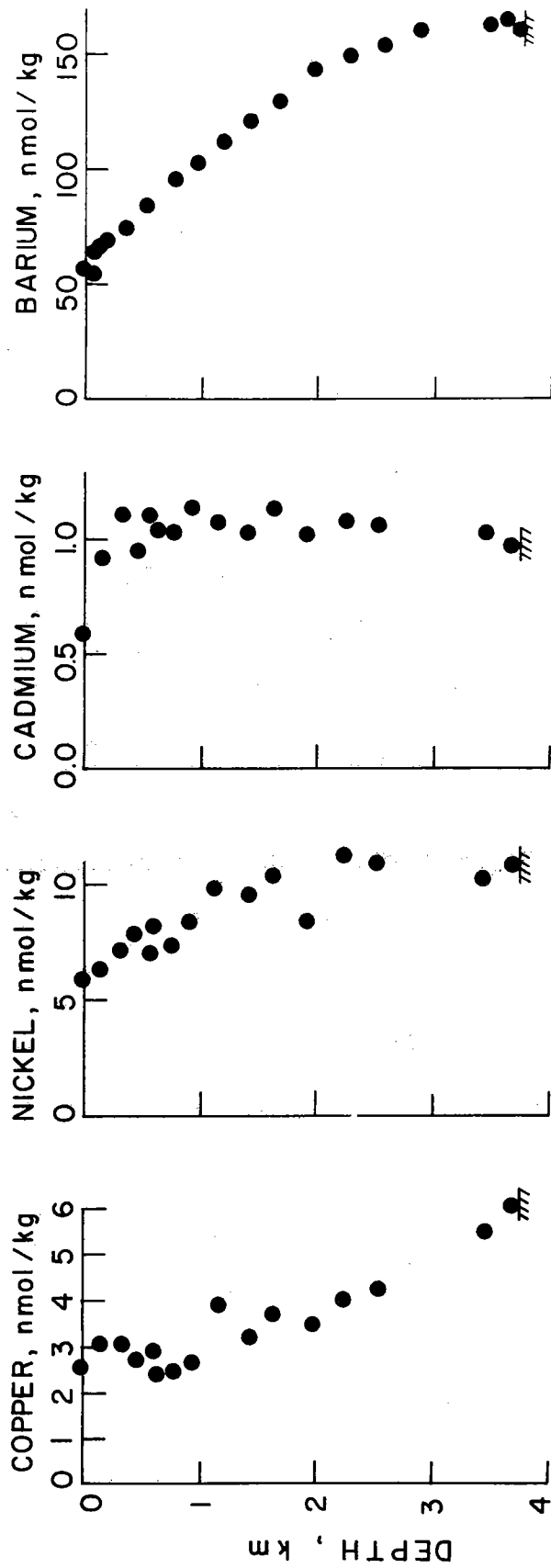
organic tissue as well as rapidly-dissolving hard parts

such as the celestite tests of Acantharia (1,2). Similarly,

metals could be carried into the deep ocean in either

carbonate or silicate tests. In fact the metals could be

incorporated into presently uncharacterized phases; the

only constraint is the rate at which the different metals

are recycled.

The first step in the metal cycle is uptake by living

organisms. Two lines of evidence bear on the laws governing

this process. Documentation is not yet extensive, however,

so that conclusions based on these observations must be

viewed with caution.

(1) The cadmium concentration of plankton appears to

be proportional to the cadmium concentration of the water

in which the organisms live. Martin and Broenkow (3)

observed 3x enrichments of cadmium in an upwelling region

relative to regions of lower productivity. The effect did

not appear to be related to variations in species composition

(3). The cadmium concentrations in that upwelling region

are estimated to be enriched by a similar factor (chapter 4).

Cossa (4) observed that cadmium could be removed rapidly

from cultured diatoms by addition of a complexing agent

(cysteine) to the culture medium. These observations

suggest that organisms maintain a reversible "equilibrium"

cadmium content dependent on the thermodynamic activity

of cadmium in the surrounding water. In the ocean the

cadmium activity is directly proportional to the total

concentration (5), so to a first approximation the

behavior of organisms with respect to cadmium can be

modeled as

$$\frac{(Cd) \ Organism}{(Cd) \ Water} = K.$$

Cadmium in plankton is thus quite labile and it is not

surprising that it is regenerated in a shallow cycle.   A

similar law may apply to that fraction of the nickel

also involved in shallow regeneration.

(2)   Barium and copper show no evidence of a shallow

regeneration component in their profile distributions.   If

some fraction of these elements in organisms is engaged in

a labile equilibrium as is cadmium, the amount must be

small relative to the total metal concentration

in the sinking particulates.   Organisms must place these

metals in sites that are only slowly recycled,although it

is conceivable that there may also be other sites so rapidly

recycled that no significant vertical transport occurs.

Consequently the uptake laws are likely to be different for

these elements than that of cadmium.

Based on the systematics of the barium distribution

in the ocean, Edmond (personal communication) proposed that

the barium uptake by siliceous organisms was governed by the

relation

$$\left(\frac{Ba}{Si}\right)_{Organism} = \alpha \ \left(\frac{Ba}{Si}\right)_{Water}$$

where α is a constant. Subsequently Ng (6) demonstrated
that this relation was consistent with her data on barium
uptake in diatom cultures and data on water and plankton
from Walvis Bay. In the experimental and field results
the variations in the Ba/Si ratio were dominated by changes
in the silica concentration of the water (10x) as only small
variations in the barium concentration (2x) were encountered.
Thus in these data the Ba/Si ratio in the organisms is
definitely inversely proportional to the silica concentration
in the water.

Silica uptake by diatoms has been shown to be
approximated by the relation

$$\frac{1}{n} \frac{dSi}{dt} = \frac{V_{max}[Si]}{K + [Si]}$$

where n is the number of cells per liter, V_{max} is the
maximum uptake rate (at high silica concentrations), K
is a constant, and all other parameters are held constant
(7). Once incorporated into the test the rate of re-release
by dissolution is low. At low silica concentrations
(< 5 μm/kg) the uptake law can be approximated as a
linear relation

$$\frac{1}{n} \frac{dSi}{dt} = k_{Si}[Si]$$

If the equation proposed by Edmond is generally valid,
the corresponding barium uptake law must be

$$\frac{1}{n} \frac{dBa}{dt} = k_{Ba}[Ba]$$

In other words, the rate of uptake of barium is independent of the silicate concentration and hence of the growth rate of the cells, within the range of growth rates where the above relations are valid. This rather surprising result is plausible if the organisms continually place barium into a refractory site that does not significantly interact with the internal environment of the cell or the growth medium. The kinetic uptake law and the observed deep regeneration both may be consequences of the site of incorporation of barium. Similar conclusions may apply to other metals that are regenerated in a deep cycle, such a copper and the deep component of nickel.

Organisms have evolved a highly selective system for processing essential nutrient elements. It is not surprising that similarly selective mechanisms exist for trace metals. This internal processing by organisms has been shown here to control a large degree of the variations observed for copper, nickel, and cadmium in the ocean. An understanding of the uptake mechanisms can lead to a broad understanding of the rates of removal of trace metals from the surface ocean, their subsequent regeneration cycles at depth and the processes controlling their distribution in the sediments.

References

(1) Brass, G.W. and K.K. Turekian (1974), Strontium distribution in Geosecs Oceanic Profiles, Earth Plan. Sci. Letters, 23:141-148.

(2) Bishop, J., J. Edmond, D. Ketten, M. Bacon, and W. Silker (1976), The chemistry, biology, and vertical flux of particulate matter from the upper 400 m of the equatorial atlantic ocean, submitted to Deep Sea Research.

(3) Martin, J. and W.W. Broenkow (1975), Cadmium in plankton: elevated concentrations off Baja California, Science 190:884-885

(4) Cossa, D. (1976), Sorption du cadmium par une population de la diatomee Phaeodactlyum triconutum en culture, Marine Biology 34:163-167

(5) Zirino, A. and S. Yamamoto (1972), A pH-dependent model for the speciation of copper, zinc, cadmium, and lead in seawater, Limnol. Oceanogr. 17:661-671

(6) Ng, A. (1975), Barium uptake by diatoms and the ^{226}Ra-Ba-Si system in the ocean, M.S., Massachusetts Institute of Technology.

(7) Passhe, E. (1973), Silicon and the ecology of marine plankton Diatoms. II. Silicate-uptake kinetics in five diatom species, Marine Biology 19:262-269.

BIOGRAPHICAL NOTE

The author was born on May 1, 1949, in Aberdeen, Maryland. He grew up in numerous localities and graduated from San Leandro High School in June 1967. In September, 1967 he entered the University of California, San Diego, where he received a B.A. degree in chemistry (highest honors) in June, 1971. In July, 1971 he entered the M.I.T.-W.H.O.I. Joint Program in Oceanography as a candidate for the degree of Doctor of Philosophy.

Publications

1971

Jolly, W.L. and E.A. Boyle, Coulometric Potentiometric Titrations of Weak Acids in Liquid Ammonia, Anal. Chem. 43:514-518.

Jolly, W.L., E.A. Boyle, and M.L. Javet, The use of indicators in acid-base titrations in liquid ammonia, J. Inorg. Nucl. Chem. 33:783-789.

1974

Boyle, E., R Collier, A.T. Dengler, J.M. Edmond, A.C. Ng, and R.F. Stallard, On the Chemical Mass Balance in Estuaries, Geochim. Cosmochim. Acta 38: 1719-1728.

1975

Boyle, E. and J.M. Edmond, Copper in surface waters south of New Zealand, Nature 253: 107-109.

Milliman, J. and E. Boyle, Biological uptake of dissolved silica in the Amazon River Estuary, Science 189:995-997.

Boyle, E. and J.M. Edmond, Determination of Trace Metals in Aqueous Solution by APDC Chelate Coprecipitation, in: Analytical Methods in Oceanography (ed. Gibb) Advances in Chemistry Series #147 , American Chemical Society, Washington D.C., p. 44-55.

Accepted for publication: Sclater, F. R., E. A. Boyle and J. M. Edmond, On the marine geochemistry of nickel, Earth Plan. Sci. Lett., in press.